U.S. DEPARTMENT OF COMMERCE

PB80-166911

New Liquid Chromatographic Detection System for Environmental Pollutants

Georgia Univ, Athens Dept. of Chemistry

Prepared for

Environmental Research Lab.
Athens, GA

Feb 80

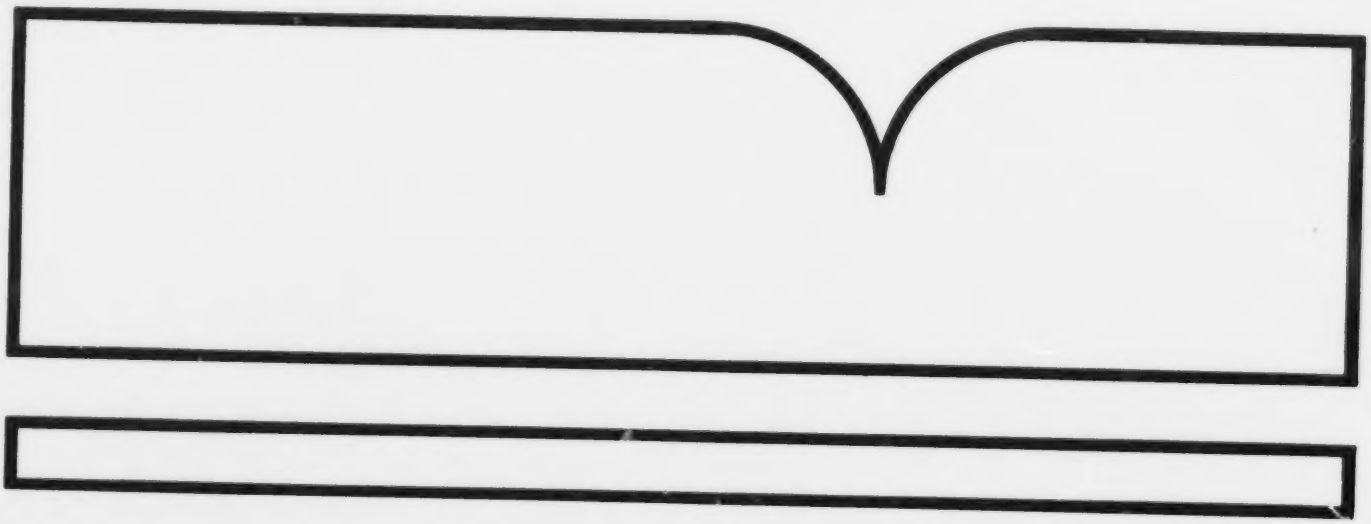

U.S. Department of Commerce
National Technical Information Service
NTIS

United States
Environmental Protection
Agency

Environmental Research
Laboratory
Athens GA 30605

EPA-600/4-80-015
February 1980

PB80-166911

Research and Development

EPA

New Liquid Chromatographic Detection System for Environmental Pollutants

REPRODUCED BY
NATIONAL TECHNICAL
INFORMATION SERVICE
U. S. DEPARTMENT OF COMMERCE
SPRINGFIELD, VA. 22161

RESEARCH REPORTING SERIES

Research reports of the Office of Research and Development, U.S. Environmental Protection Agency, have been grouped into nine series. These nine broad categories were established to facilitate further development and application of environmental technology. Elimination of traditional grouping was consciously planned to foster technology transfer and a maximum interface in related fields. The nine series are:

1. Environmental Health Effects Research
2. Environmental Protection Technology
3. Ecological Research
4. Environmental Monitoring
5. Socioeconomic Environmental Studies
6. Scientific and Technical Assessment Reports (STAR)
7. Interagency Energy-Environment Research and Development
8. "Special" Reports
9. Miscellaneous Reports

This report has been assigned to the ENVIRONMENTAL MONITORING series. This series describes research conducted to develop new or improved methods and instrumentation for the identification and quantification of environmental pollutants at the lowest conceivably significant concentrations. It also includes studies to determine the ambient concentrations of pollutants in the environment and/or the variance of pollutants as a function of time or meteorological factors.

This document is available to the public through the National Technical Information Service, Springfield, Virginia 22161.

TECHNICAL REPORT DATA
(Please read Instructions on the reverse before completing)

1. REPORT NO.	2.	3. RECIP
EPA-600/4-80-015		PB80 166911

4. TITLE AND SUBTITLE	5. REPORT DATE
New Liquid Chromatographic Detection System for Environmental Pollutants	February 1980 issuing date
	6. PERFORMING ORGANIZATION CODE
7. AUTHOR(S)	8. PERFORMING ORGANIZATION REPORT NO.
L.A. Carreira and L.B. Rogers	
9. PERFORMING ORGANIZATION NAME AND ADDRESS	10. PROGRAM ELEMENT NO.
Department of Chemistry University of Georgia Athens, Georgia 30602	A37B1D
	11. CONTRACT/GRANT NO.
	R804155-03-0
12. SPONSORING AGENCY NAME AND ADDRESS	13. TYPE OF REPORT AND PERIOD COVERED
Environmental Research Laboratory--Athens GA Office of Research and Development U.S. Environmental Protection Agency Athens, Georgia 30605	Final, 1/76-12/78
	14. SPONSORING AGENCY CODE
	EPA/600/01

15. SUPPLEMENTARY NOTES

16. ABSTRACT

Resonance enhanced coherent anti-Stokes Raman spectrometry (CARS) has been demonstrated as a specific identification system for liquid chromatography. To achieve this, liquid chromatographic preconcentration and separation and computer control of the liquid chromatograph/ultraviolet-visible/CARS were undertaken. Under the optimum resonance condition, spectra were obtained on 5 microliter volumes with detection limits of 1 micromolar or less under favorable conditions. Excellent fluorescence rejection and ultraviolet CARS were also shown. A number of different species were surveyed by liquid chromatography with the selectivity of different stationary phases and special solvent effects examined. Observations useful in relating experimental variables in the preconcentration step to the recovery of a given species were made. A system consisting of a liquid chromatograph, a scanning ultraviolet-visible spectrometer and the CARS was automated using a minicomputer. Column selection, flow rate, and solvent composition were monitored and controlled. The ultraviolet-visible spectrometer was used at a fixed wavelength until a species was detected. The flow was stopped, the absorption spectrum was scanned, and flow was resumed. The optimum laser frequencies for resonance CARS were set from the absorption spectrum. The Raman spectra were then scanned under control of the computer with on-line signal averaging and data smoothing.

17. KEY WORDS AND DOCUMENT ANALYSIS

a. DESCRIPTORS	b. IDENTIFIERS/OPEN ENDED TERMS	c. COSATI Field/Group
Chemical analysis Chromatography Spectrometers		07B 68D

18. DISTRIBUTION STATEMENT	19. SECURITY CLASS *(This Report)*	21. NO. OF PAGES
RELEASE TO PUBLIC	UNCLASSIFIED	
	20. SECURITY CLASS *(This page)* UNCLASSIFIED	22. PRICE

☆ U.S. GOVERNMENT PRINTING OFFICE 1980-657-146/5591

EPA-600/4-80-015
February 1980

NEW LIQUID CHROMATOGRAPHIC DETECTION SYSTEM FOR ENVIRONMENTAL POLLUTANTS

by

L. A. Carreira and L. B. Rogers
University of Georgia
Athens, Georgia 30602

Grant No. R804155-03-0

Project Officer

Leo Azarraga
Analytical Chemistry Branch
Environmental Research Laboratory
Athens, Georgia 30605

ENVIRONMENTAL RESEARCH LABORATORY
OFFICE OF RESEARCH AND DEVELOPMENT
U.S. ENVIRONMENTAL PROTECTION AGENCY
ATHENS, GEORGIA 30605

i.a

DISCLAIMER

This report has been reviewed by the Environmental Research Laboratory, Athens, Georgia, and approved for publication. Approval does not signify that the contents necessarily reflect the views and policies of the U.S. Environmental Protection Agency, nor does mention of trade names or commercial products constitute endorsement or recommendation for use.

FOREWORD

Nearly every phase of environmental protection depends on a capability to identify and measure specific pollutants in the environment. As part of this Laboratory's research on the occurrence, movement, transformation, impact and control of environmental contaminants, the Analytical Chemistry Branch develops and assesses new techniques for identifying and measuring chemical constituents of water and soil.

Early in the development of gas chromatography-Fourier transform infrared spectroscopy methods at this Laboratory, the need for an on-line spectroscopic technique to measure vibration spectra of liquid chromatographic eluates was recognized. One of the responses to this need was the funding of a project to develop the coherent anti-Stokes resonance Raman spectroscopy liquid chromatography system. This report describes the development of such a system, which should prove useful in the analysis of relatively nonvolatile organic compounds.

David W. Duttweiler
Director
Environmental Research Laboratory
Athens, Georgia

ABSTRACT

Resonance enhanced coherent anti-Stokes Raman spectrometry (CARS) has been demonstrated as a specific identification system for liquid chromatography. To achieve this work in the areas of CARS, liquid chromatographic preconcentration and separation and computer control of the liquid chromatograph/ultraviolet-visible/CARS experiments were undertaken.

Under the optimum resonance condition for CARS, spectra have been obtained on five microliter volumes with detection limits of one micromolar or less under favorable conditions. Excellent fluorescence rejection and ultraviolet CARS have also been shown.

A number of different species have been surveyed by liquid chromatography with the selectivity of different stationary phases and special solvent effects examined. Observations useful in relating experimental variables in the preconcentration step to the recovery of a given species have been made.

A system consisting of a liquid chromatograph, a scanning ultraviolet-visible spectrometer and the CARS experiment have been automated using a DEC PDP 11/34 minicomputer. Column selection, flow rate, and solvent composition were monitored and controlled. The ultraviolet-visible spectrometer was used at a fixed wavelength until a species was detected. The flow was stopped, the absorption spectrum was scanned, and flow was resumed. From the absorption spectrum the optimum laser frequencies for resonance CARS were set along with the proper crossing angle, detector stage angle, and monochromator wavelength for the Raman signal. The Raman spectra was then scanned under control of the computer with on-line signal averaging and data smoothing.

This report was submitted in fulfillment of Grant No. R804155-03-0 by the University of Georgia under the sponsorship of the U. S. Environmental Protection Agency. This report covers the period January 1, 1976 to December 31, 1978, and work was completed as of December 31, 1978.

CONTENTS

Foreword iii

Abstract iv

Figures vi

Tables xi

Executive Summary xii

Acknowledgments xvi

1. Introduction 1
2. Conclusions 3
3. Recommendations 5
4. Liquid Chromatography 6
   - General Apparatus 6
   - Chemicals and Packing Materials 7
   - Separation of Polynuclear Aromatic Hydrocarbons (PAH) and Aroclor 1242 on a C_{18} Column 7
   - Retention Behavior of Dinitrobenzene (DNB) and Dihydroxybenzene (DHB) Isomers on Phenyl-Bonded Phase Columns 9
   - Comparison of Two Recovery Methods on Bonded Phase Packings .. 16
   - Effect of Change in Solvent on Chromatographic Peak Shapes 18
   - Comparison of the Recovery on Two Different Bonded Phases 19
5. Coherent Anti-Stokes Raman Spectroscopy 21
   - Introduction to CARS 21
   - Initial Setup and Solvent Studies 23
   - Sample Cell Development 23
   - Signal Enhancement in the Rigorous Resonance Region 24
   - Photomultiplier Detection 33
   - Raman Spectra of Fluorescent Compounds 34
   - UV Experiments 35
   - Lineshapes in CARS Spectra 36
   - Preresonance Enhancement of Fluorescent Compounds 37
   - Resonance Enhancement of Fluorescent Compounds Near Their Absorption Maximum 38
6. Computer Interfaces 43

References 51

Collaborators and Publications 53

FIGURES

Number		Page
1	Chromatogram of nine polynuclear aromatic hydrocarbons using Lichrosorb RP 18 packing and isocratic elution. Column: 30 cm x 0.5 cm i.d., Lichrosorb RP18, 10μ; solvent composition: 80% methanol/ 20% water; flow rate: 1 ml/min; temp: ambient; detector: UV (254), 0.1 absorbance, full scale	8
2	Chromatogram of 42% chlorinated biphenyls (Aroclor 1242) using Lichrosorb RP 18 packing and gradient elution. Column: 30 cm x 0.5 cm i.d., Lichrosorb RP 18, 10μ ; mobile phase, linear gradient: 30% methanol/70% water to 80% methanol/ 20% water; gradient time: 60 min; temp: ambient; flow rate: 1.5 ml/min; detector: UV (254), 0.1 absorbance, full scale	9
3	Separation of dinitrobenzene isomers on the phenyl-bonded phase packing at different solvent composition. Column: 60 cm x 0.5 cm i.d., Phenyl Bondpak/Porasil B, 37 ~ 75μ; temp: ambient; detector: UV (254), 0.1 absorbance, full scale	11
	(A) Solvent composition: 20% methanol/80% water for the first 120 minutes and 45 % methanol/55% water after 120 minutes; flow rate: 4.5 ml/min	
	(B) Solvent composition: 35% methanol/65% water; flow rate: 3 ml/min	
	(C) Solvent composition: 60% methanol/40% water; flow rate: 2 ml/min	
4	Separation of dinitrobenzene isomers on the octadecyl-bonded phase packing at different solvent composition. Column: 30 cm x 0.5 cm i.d., Lichrosorb RP 18, 37 ~ 75μ; temp: ambient; detector: UV (254), 0.1 absorbance, full scale	12
	(A) Solvent composition: 20% methanol/80% water; flow rate: 3 ml/min	
	(B) Solvent composition: 35% methanol/65% water; flow rate: 2 ml/min	

Number		Page
	(C) Solvent composition: 60% methanol/40% water flow rate: 1 ml/min	
5	Comparison of the separations of dinitrobenzene isomers on two different bonded phase packings under the same condition except the particle size. Column: 30 cm x 0.5 cm i.d., temp: ambient; flow rate: 2 ml/min; solvent composition: 45% methanol/55% water; detector: UV (254), 0.1 absorbance, full scale	13
	(A) The octadecyl-bonded phase (Lichrosorb RP 18), particle size: 10 μ	
	(B) The phenyl-bonded phase (Phenyl Bondpak/Porasil B), particle size: 37 ~ 75 μ	
6	Separation of dihydroxybenzene isomers on the phenyl-bonded phase packing at different solvent composition. Column: 60 cm x 0.5 cm i.d., Phenyl Bondpak/Porasil B, 37 ~ 75 μ; temp: ambient; detector: UV (254), 0.1 absorbance, full scale	14
	(A) 30% methanol/70% water; flow rate: 2 ml/min	
	(B) 15% methanol/85% water; flow rate: 2 ml/min	
	(C) 5% methanol/95% water; flow rate: 2.5 ml/min	
	(D) 0% methanol/100% water; flow rate: 2.5 ml/min	
7	Separation of dihydroxybenzene isomers on the octadecyl-bonded phase packing. Column: 30 cm x 0.5 cm i.d., Lichrosorb RP 18, 10μ; temp: ambient; detector: UV (254), 0.1 absorbance, full scale; flow rate: 2 ml/min; solvent composition: 100% water	15
8	A portion of the preresonance coherent anti-Stokes Raman spectrum of trans-beta-carotene. ω_1 is 575 nm. The concentration is 10^{-3} M	25
9	Observed (...) and calculated (solid line) CARS excitation profile for the ν_1 vibrational mode of beta-carotene	28
10	Observed (...) and calculated (solid line) CARS excitation profile for the ν_2 vibrational mode of beta-carotene	29
11	Calculated spontaneous Raman excitation profile for the ν_1 vibration of beta-carotene using the same parameters as in Figure 3	30

Number		Page
12	Calculated spontaneous Raman excitation profile for the ν_2 vibration of beta-carotene using the same parameters as in Figure 4	31
13	Plot of the log of the power in ω_1 versus the log of the power in ω_3 for trans-beta-carotene (·) and benzene (O)	32
14	Preresonance CARS spectrum of beta-carboline	34
15	Preresonance CARS spectrum of beta-naphthol	35
16	UV-CARS spectrum of the CH stretch region in methanol	36
17	Automated UV-CARS spectrum of toluene	37
18	CARS spectrum of perylene in benzene taken at a pump wavelength of 450 nm. The quantum efficiency of fluorescence for this compound is .94	39
19	CARS spectrum of rhodamine 6G in ethanol taken at a pump wavelength of 535 nm. The quantum efficiency of fluorescence for this compound in ethanol is .95	39
20	CARS spectrum of rhodamine B in ethanol taken at a pump wavelength of 555 nm. The quantum efficiency of fluorescence for this compound in ethanol is .40	40
21	CARS spectrum of sodium fluorescein in water at an alkaline pH taken at a pump wavelength of 510 nm. The quantum efficiency of fluorescence for this compound is .90	40
22	CARS spectrum of acridine orange in water at a pump wavelength of 510 nm. The quantum efficiency of fluorescence for this compound is above .50	41

Number		Page
23	CARS spectrum of coumarin 495 in ethanol at a pump wavelength of 425 nm. The quantum efficiency of fluorescence for this compound is above .70	41
24	Excitation profiles for the ring breathing mode of tetracene as a function of the pump wavelength and displacement parameter. The solid lines represent the theoretical profile at various displacement parameters. The circles represent the experimentally obtained values	42
25	Experimental CARS setup used in the studies	44
26	Schematic of the peripheral bus (peribus) used to extend the number of possible I/O ports. The symbols are: OB - output bit, DA - data available, DT - data transmit, IB - input bit and REQ - request. The pull up resistors are 1 k. The resistor-capacitor circuit employed a 51 k resistor and a 560 pF capacitor	45
27	Simplified schematic of the basic operation of the scan unit interface. Both the input and output ports of the DR11k were required for communication with the computer	46
28	Simplified schematic of the basic operation of the stepping motor interface. The DR11C I/O port was used for controlling this interface	47
29	More detailed schematic of the stepping motor interface under local and computer control	48

Number		Page
30	Schematic of the actual circuit used for the stepping motor interface. The symbols are: OWØ - output word bit Ø, SA - computer/local switch, SB - direction switch, SC - scan switch, SD - single step switch, OSC - oscillator, MS1 - limit micro-switch for the CW direction and RUN turns on an external oscillator	49

TABLES

Number		Page
1	Elution orders of dinitrobenzene isomers on the octadecyl and the phenyl bonded phase packings using different solvent compositions	10
2	Results of recovery studies on the C_{18} column using two different methods	17
3	Results of recovery studies of some compounds by injection method using two different packings	20

EXECUTIVE SUMMARY

The goal of this research was to explore the use of resonance enhanced coherent anti-Stokes Raman spectrometry (CARS) as the basis for a specific identification system for liquid chromatography. The overall system, which also includes a liquid chromatograph and a UV-visible spectrometer, not only provides sensitive detection but also multiple means of identification through retention times (volumes), UV-visible absorption spectra, and vibrational Raman spectra.

Work was concentrated in these areas: CARS spectroscopy, liquid chromatographic preconcentration and separation, and computer control of the LC/UV-visible/CARS experiments. The overall goal has been accomplished successfully, and we have demonstrated using a model chemical sample that the system is capable of: (a) separating a complex mixture using liquid chromatography, (b) detecting individual components at a fixed, preselected wavelength, (c) obtaining the entire absorption spectrum near the point of maximum absorption using a stopped-flow mode, (d) analyzing that spectrum to determine the optimum condition for exciting the Raman spectrum, (e) starting the flow to pass the solution from the absorption cell to the Raman emission cell, and (f) stopping the flow once again to obtain the anti-Stokes Raman spectrum under optimum resonance conditions. Steps (b) to (f) can be completed in approximately 10 minutes per species. By starting the flow once again, successive species eluting from the liquid chromatograph can be characterized.

Now that the feasibility of the system has been demonstrated, one can easily predict how to modify the existing system so as to reduce the time required to characterize the single species in less than two minutes. In addition,

one can predict that the versatility of the system could be expanded to include other types of measurements.

The bases of those predictions can best be understood by following the stepwise developments that occurred during the past three years. In the CARS area, it was first necessary to purchase the powerful lasers and assemble the spectrometer. Using only manual adjustments, an approach for attaining the optimum resonance condition was developed following which it was possible to show that spectra could be obtained on volumes of less than five microliters while at the same time having a detection limit under favorable circumstances of less than one micromolar. Furthermore, low limits were obtained using highly fluorescent compounds, e.g., rhodamine 6G, thereby demonstrating good rejection of unwanted fluorescence. In addition, it was found that laser power had to be decreased when working with very dilute solutions so as to avoid saturation of the excited state. Finally, work was extended into the ultraviolet range.

In chromatography a number of different species were surveyed but most of the effort was devoted to comparing selectivities of different packing materials and exploring special solvent effects. For example, if the sample is dissolved in one solvent and eluted from the chromatographic column using a second, a single substance was sometimes found to produce two peaks instead of one. Finally, observations were made relating experimental variables in the preconcentration step to the recovery of a given species.

The final step involved overall automation of a system that consisted of a liquid chromatograph, a scanning ultraviolet-visible spectrophotometer, and the Raman spectrometer. In order to speed up the process of interfacing as well as to increase its flexibility, a modular approach was taken.

Furthermore, the designs were such that control and data acquisition could be easily effected using the real-time Fortran provided by the Digital Equipment Corporation for its PDP 11/34 minicomputer.

With respect to the liquid chromatograph, the system permitted selection between two columns so that, if desired, a sample could be preconcentrated in one column and then moved to a second column for analysis. In addition, operating parameters such as flow rate of the eluent, solvent composition, and temperature could be monitored and controlled.

A UV-visible spectrophotometer was set at a pre-selected wavelength in order to be used as a detector. Shortly after the maximum absorption for a species had been detected, the flow was stopped and the spectrophotometer was scanned in order to obtain a spectrum. After the flow had been resumed, the absorption continued to be measured so that the peak could be integrated for quantitative purposes.

Meanwhile, from the ultraviolet-visible spectrum, the optimum wavelength was calculated for exciting the Raman emission. After the optimum pumping frequencies had been set, mirror positions were adjusted so as to obtain the proper crossing angles and the emission was directed at a spectrometer that served to reject stray light, including that from fluorescence. The latter was done by adjusting the angle of the detector relative to the sample cell. It is important to note that the computer adjusted the instrument before each measurement.

The software was developed independently for each major function for controlling each of the instruments, for detecting and integrating chromatographic peaks, and for calculating results such as those for the optimum

wavelength for irradiation. In addition, there was on-line signal-to-noise enhancement using signal averaging and statistical treatment of data to reject out-lying results. Finally, there was digital smoothing and plotting of data.

ACKNOWLEDGMENTS

The helpful discussions with Dr. Leo Azarraga, Environmental Protection Agency, Office of Research and Development, Environmental Research Laboratory, Athens, Georgia, are gratefully acknowledged.

SECTION 1

INTRODUCTION

There is a rapidly growing need for detection systems for liquid chromatography (LC) that provide a capability comparable to that obtained from the combination of a gas chromatograph with a mass spectrometer. Although attempts have been made to adapt mass spectrometry to liquid chromatography, that marriage is an unrealistic one in the sense that liquid chromatography can best be used (in preference to gas chromatography) for compounds that are unstable to heat or are non-volatile. While those compounds can sometimes be handled by adding another step, such as derivatization or pyrolysis, extra work is required, and the capability for on-line detection and quantitation is usually lost. Furthermore, the question of how quantitatively or reproducibly the derivatization or pyrolysis can be done has often been a limiting factor. Hence, a direct analysis is highly desirable.

A major goal of our work has been to make a detailed evaluation of coherent anti-Stokes resonance Raman spectroscopy using relatively non-volatile organic compounds, mostly aromatics, that are typical of those encountered in different phases of coal utilization and in the pesticide-insecticide area.

Since the coherent anti-Stokes Raman signal can be measured with little interference from fluorescence because: (a) the CARS signal occurs at a higher energy than the excitation (whereas fluorescence occurs at a lower energy) and (b) the fluorescence is emitted in all directions so the fraction in the small solid angle occupied by the spatially coherent CARS signal will be very small. We have been able to record CARS spectra of molecules whose fluorescence would prohibit their measurement using the spontaneous Raman effect.

As will be shown later, use of resonance conditions along with ordinary CARS enhancement has pushed the detection limits for many compounds below the micromolar level. In order to achieve this level of detection, much has been done to optimize cell design and to determine solvent limitations on the detection of very dilute solutes.

Since most molecules of interest will have absorptions in the UV region of the spectrum, it was advantageous to carry out resonance enhancement studies in this range. By using a frequency doubling technique and photomultiplier detection, we have been able to record strong CARS signals in the CH stretch region of the polar methanol molecule.

SECTION 2

CONCLUSIONS

Our results indicate that coherent anti-Stokes Raman spectroscopy (CARS) may be used as a specific detector for liquid chromatography (LC). The two major problems involved in applying CARS as a specific LC detector have been overcome. The small internal volume (1 to 10 microliters) requirement has been solved by using capillary cells. Based on the shape (cylindrical) and inside diameter (1.2 mm), we have calculated and experimentally verified that flow rates as high as two meters per second can be used without turbulent flow disturbing the beams. This is over an order of magnitude faster than a fast LC flow rate.

The second problem of being able to detect species at concentrations of 10^{-5} to 10^{-6} M has also been solved. The previous drawback to using CARS for low concentrations had been the fact that the solute signal was obscured by the strong non-resonant background signal of the solvent and allowed lower limits of detection of only 5×10^{-2} M. The solution was to increase the solute signal over the solvent signal by pumping the system with a frequency resonant absorption frequency of the solute. This adjustment increased the relative power of the solute signal by several orders of magnitude and has allowed solute detection at concentrations of 5 to 7 M. This has allowed empirical establishment of the lower molar limit of detection by CARS to be $(10 \cdot E)^{-1}$ M where E is the decadic molar absorption coefficient of the solute.

In order to apply the resonance enhancement technique to a wide range of compounds, it is necessary to be able to pump in the ultraviolet region of the spectrum. We have shown that by using frequency

doubling techniques we can obtain UV beams of sufficient intensity to produce strong CARS signals. This means that the CARS technique will be applicable for a great number of compounds of interest.

In the liquid chromatographic studies, a phenol-derivatized silica packing was found to be more selective than a C_{18}-derivatized packing for highly polar aromatics, so it should provide better chromatographic separations of polar pollutants in water. In addition, an injection method for testing recovery, in which the enriched sample is dissolved in one solvent and then eluted with a second suitable solvent has proven to be an easy, fast approach for testing the relative recoveries of water pollutants. In a related study, double peaks for a single component were found under some conditions when two solvents were employed. Finally, preliminary schemes have been developed for the liquid chromatographic separation of polynuclear aromatics and polychlorinated biphenols. The separations of components were usually large enough to allow individual species to be investigated by CARS.

The design of the computer interface has been based on a modular approach. This design allowed the development of each controlled experimental function as a unit. Each unit can be addressed individually using the software. The overall result is that, by using this apparatus one can now obtain a much better (i.e., higher S/N) CARS spectrum in six minutes than one could obtain in two hours by manual operation. It is now possible to characterize isolated solute peaks (both UV-visible absorption and Raman emission) in approximately 10 minutes. The only additional time is that required for the chromatographic fractionation itself.

SECTION 3

RECOMMENDATIONS

Now that the basic approach has been demonstrated to be feasible, one can predict how parts of the development process could be speeded up. First, both UV-visible absorption and Raman emission could be measured on a time-scale smaller by a factor of 10 by using vidicon (multi-cathode) detectors. Those detectors permit simultaneous measurements to be made over a relatively wide range of wavelengths. Second, the system could also be made much more compact by using newer, smaller lasers having equivalent power. Hence, a more manageable, table-top unit could be constructed by a user who wishes to duplicate the present capability.

SECTION 4

LIQUID CHROMATOGRAPHY

Our main efforts in the liquid chromatographic study can be described in three different areas. First, quantitative separations of water pollutants are the chief goal. In the past, different absorbents such as XAD resins and charcoal[1-3] have been used for preconcentration. Recently, an on-column method based on a C_{18} column has been developed[4] for both concentration and separation. The second area involved in our studies was to characterize the phenyl-bonded phase which has not yet been used by others. We have studied dinitrobenzene and dihydroxylbenzene isomers.

Besides separation, the efficiency of the column to collect these trace organics from water is very important for the present project. Therefore, the third area covered in our studies was the recovery of the sample from a given column. The recovery efficiencies of the C_{18} and the phenyl-bonded phase packings were compared for some aromatic compounds. In this study, both the pumping method and the injection method were used.

GENERAL APPARATUS

The liquid chromatograph used for the present work is a Micromeritics Model 7000 B. This instrument is equipped with a 6000 psi solvent delivery system with constant flow and different gradient capabilities. It is also equipped with a UV detector operating at 254 nm. Later, a GCA McPherson, Model EU-700, UV-visible spectrophotometer was substituted for the original UV detector. Sample injections were accomplished by means of the Universal Sample Injector (Micromeritics) with 100 microliters as the maximum capacity of the sample loop.

CHEMICALS AND PACKING MATERIAL

All the chemicals used were reagent grade. Water used was deionized followed by distillation. In all cases, the mobile phase used was water, methanol, or their mixture. These solvents were degassed in an ultrasonic vibrator before use. Columns of C_{18}/porasil B and phenyl/porasil B (Waters Associates, 37-75 μm) were dry packed. Columns of Lichrosorb RP 18 (E. Merck Company, 10 μm) were packed by using the high pressure slurry method. The sample solutions, unless otherwise indicated, were prepared by dissolving each compound in methanol.

SEPARATION OF POLYNUCLEAR AROMATIC HYDROCARBONS (PAH) AND AROCLOR 1242 ON A C_{18} COLUMN

The main purpose of this portion of the study was to show the capability of new chromatographic packing for the analysis of some pollutants in water. Polynuclear aromatic hydrocarbons (PAH) and polychlorinated biphenyls were chosen for our study.

The experimental conditions in our work were very similar to what had been done in the literature[5,7]. The reverse phase mode of separation based on the C_{18} column (Lichrosorb RP 18) and water/methanol as the mobile phase were used. The column dimension was 30 cm x 0.5 cm. A UV detector was used and the attenuation was adjusted to 0.1 absorbance unit. The temperature was ambient and the chart speed of the recorder was 12 cm/hr. The flow rate in this case was adjusted to 1 ml/min and the solvent composition was made of 80% methanol and 20% water. From the above experimental condition, the separation of nine PAH compounds was achieved as shown in Figure 1. These PAH compounds were identified from their retention times.

Figure 2 is the chromatogram of Aroclor 1242 (PCB mixture) separated by the same system using gradient elution from 30% MeOH/H_2O to 80% MeOH/H_2O in 60 minutes. Here the flow rate was adjusted to 1.5 ml/min. Though each peak in this chromatogram was not identified, this separation indicates that the C_{18} column is a very efficient tool for the analysis of PCB compounds.

The CARS technique should be able to provide structural information for the above compounds. From the above separations, it is evident that

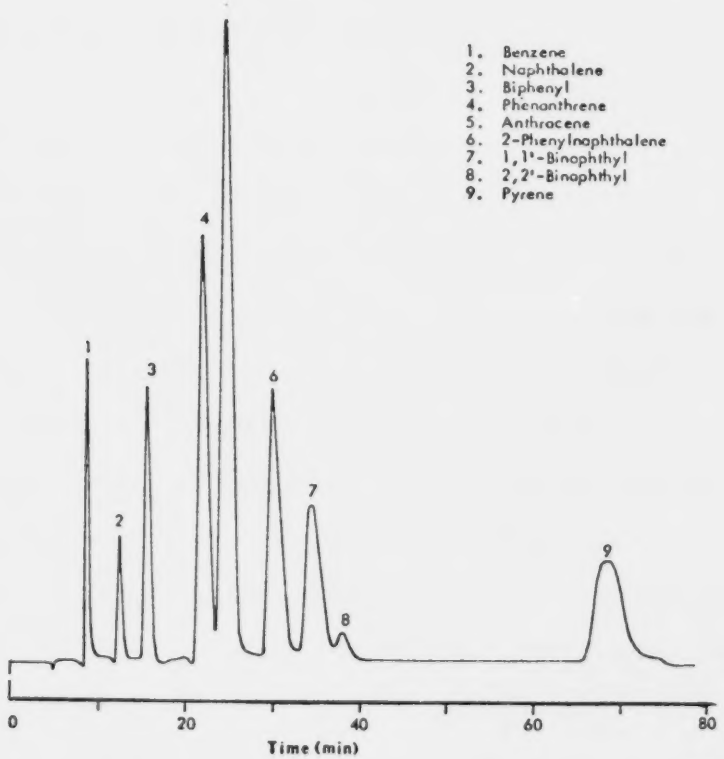

1. Chromatogram of nine polynuclear aromatic hydrocarbons using Lichrosorb RP 18 packing and isocratic elution. Column: 30 cm x 0.5 cm i.d., Lichrosorb RP 18, 10μ; solvent composition: 80% methanol/20% water; flow rate: 1 ml/min; temp: ambient; detector: UV (254), 0.1 absorbance, full scale .

the coupling of LC and CARS should be a powerful method for the monitoring of these pollutants in water. In addition, since the reverse phase mode of separation is used here, it may be possible to concentrate these pollutants and resolve them in the same column without tedious sample preparation.

RETENTION BEHAVIOR OF DINITROBENZENE (DNB) AND DIHYDROXYBENZENE (DHB) ISOMERS ON PHENYL BONDED PHASE COLUMNS

The phenyl-bonded phase is often overlooked because a much better separation of PAH can be done on the C_{18} column. However, it has been mentioned that the phenyl-bonded phase has a strong interaction with the aromatic compounds.[8] In addition, this packing material seemed to retain

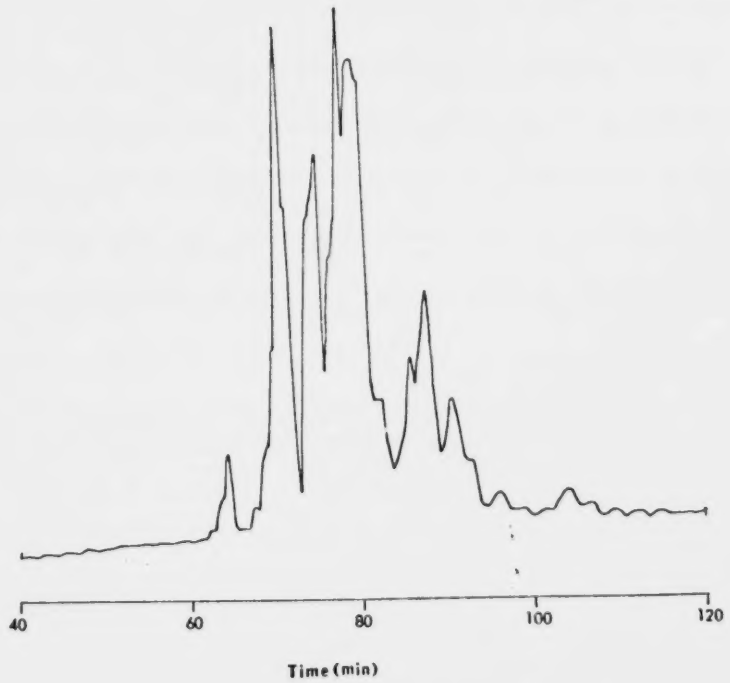

2. Chromatogram of 42% chlorinated biphenyls (Aroclor 1242) using Lichrosorb RP 18 packing and gradient elution. Column: 30 cm x 0.5 cm i.d., Lichrosorb RP 18, 10μ ; mobile phase, linear gradient: 30% methanol/70% water to 80% methanol/20% water; gradient time: 60 min; temp: ambient; flow rate: 1.5 ml/min; detector: UV (254), 0.1 absorbance, full scale.

some polar compounds longer than the C_{18} column.[8] Thus, it is of interest to determine the retention behavior on the phenyl-bond phase with some model compounds and compare it with the C_{18} column. Isomers of dinitrobenzene (DNB) and dihydroxybenzene (DHB) were chosen for this study because they are aromatic and have different polarities. Solution of these isomers were prepared in methanol just before use. The experimental setup for this study was basically the same as that described above. Both the phenyl-bonded phase and the C_{18} phase were used for the separation of DNB isomers or DHB isomers. Four different eluent compositions, 20%, 35%, 45%, and 60% $MeOH/H_2O$, were used in comparing the two bonded phases.

Results of the study of the DNB isomers are shown in Figures 3 through 5 and in Table 1. Figures 3 and 4 are the chromatograms of two columns for the separation of DNB isomers using different solvent compositions. It is interesting to note that the elution order of DNB isomers on the C_{18} column varied from one solvent composition to another while it was constant on the phenyl-bonded phase. In addition, the resolution of these DNB isomers on

Table 1. Elution orders of dinitrobenzene isomers on the octadecyl and the phenyl bonded phase packings using different solvent compositions.

	Solvent Composition % Methanol/% Water	Flow Rate (Ml/Min)	Elution Order
The octadecyl bonded phase packing, Lichrosorb RP 18	20	3	p<m<o
	35	2	p<o<m
	60	1	o<p<m
The Phenyl bonded phase packing, Bondpak Phenyl/Porasil B	20	4.5	p<m<o
	35	3	p<m<o
	60	2	p<m<o

the phenyl-bonded phase increased when the percentage of methanol decreased. This, however, was not generally true if the C_{18} column was used. Figure 5 is another comparison of these two bonded phases based on the same conditions except for the particle size. It is apparent that the phenyl-bonded phase was superior to the C_{18} column for the separation of DNB isomers even when the particle size was much larger.

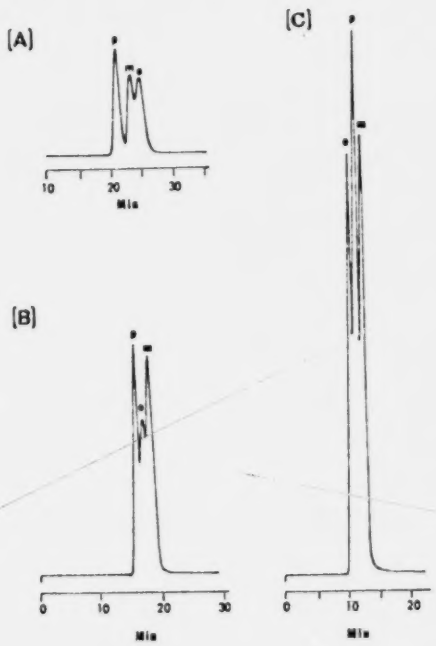

3 Separation of dinitrobenzene isomers on the phenyl-bonded phase packing at different solvent composition. Column: 60 cm x 0.5 cm i.d., Phenyl Bondpak/Porasil B, 37 ~ 75 μ; temp: ambient; detector: UV (254), 0.1 absorbance, full scale .

(A) Solvent composition: 20% methanol/80% water for the first 120 minutes and 45% methanol/55% water after 120 minutes; flow rate: 4.5 ml/min

(B) Solvent composition: 35% methanol/65% water; flow rate: 3 ml/min

(C) Solvent composition: 60% methanol/40% water; flow rate: 2 ml/min

The results of the separation of DHB isomers on these two bonded phases can be seen in Figures 6 and 7. It is interesting to note that the elution order (P<M<O) of these three isomers was the same as that of the DNB isomers when the column was the phenyl-bonded phase.

It is evident that the phenyl-bonded is a better column material for the separation of DNB isomers because of the better resolution. Unlike the C_{18} column, the elution order of these three isomers did not vary when the solvent composition changed from 60% to 15% MeOH/H_2O. This indicates

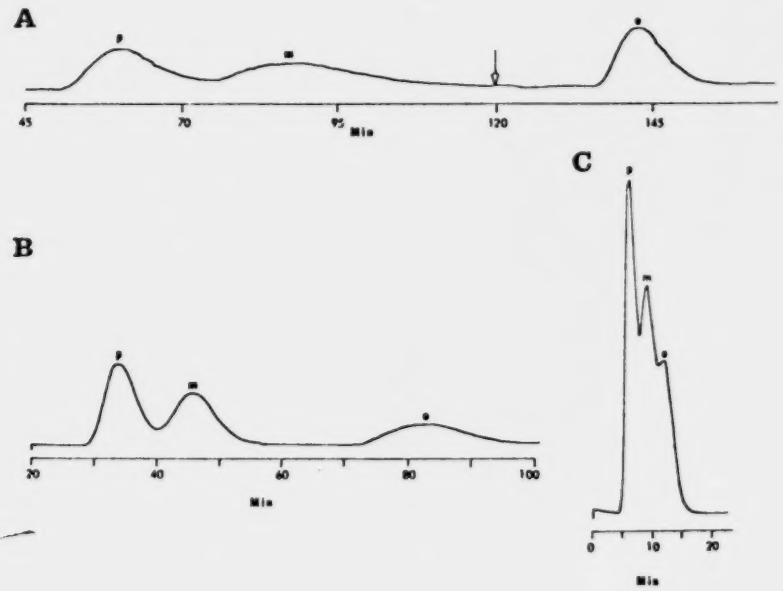

4 Separation of dinitrobenzene isomers on the octadecyl-bonded phase packing at different solvent composition. Column: 30 cm x 0.5 cm i.d., Lichrosorb RP 18, 37 ~ 75 μ; temp: ambient; detector: UV (254), 0.1 absorbance, full scale.

(A) Solvent composition: 20% methanol/80% water; flow rate: 3 ml/min

(B) Solvent composition: 35% methanol/65% water; flow rate: 2 ml/min

(C) Solvent composition: 60% methanol/40% water flow rate: 1 ml/min

a stronger interaction between the solute and the stationary phase. Further evidence can be seen from the longer retention times of these isomers compared with those from the C_{18} column under the same condition. (See Figure 5.) It is also expected that the phenyl-bonded phase packing of a smaller particle size ($5 \sim 10$ μm) will give a much better separation and much higher capacity.

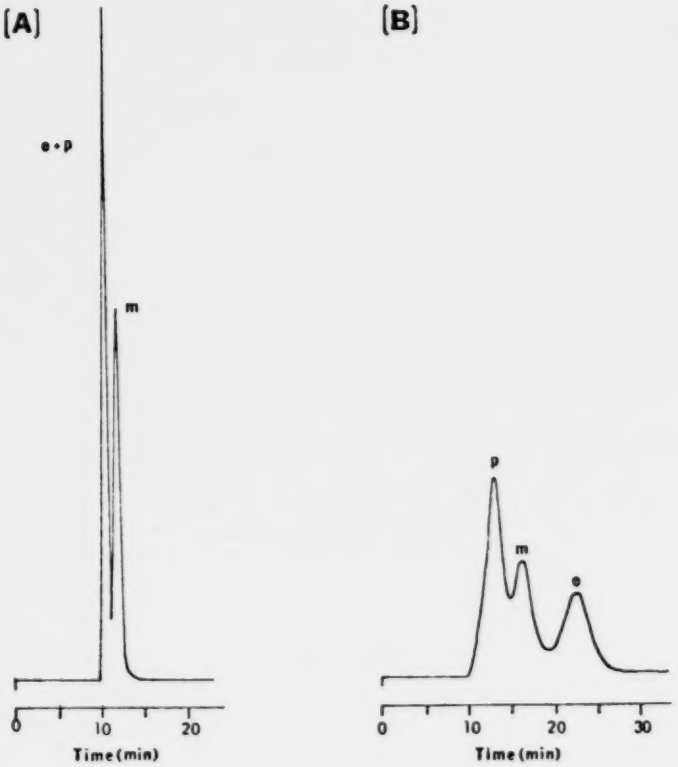

5 Comparison of the separations of dinitrobenzene isomers on two different bonded phase packings under the same condition except the particle size. Column: 30 cm x 0.5 cm i.d., temp: ambient; flow rate: 2 ml/min; solvent composition: 45% methanol/55% water; detector: UV (254), 0.1 absorbance, full scale.

(A) The octadecyl-bonded phase (Lichrosorb RP 18), particle size: 10 μ

(B) The phenyl-bonded phase (Phenyl Bondpak/Porasil B), particle size: $37 \sim 75$ μ

The separation of DHB isomers can be done by both C_{18} and the phenyl-bonded phase using the same composition of mobile phase. It is interesting that these highly polar isomers could be well separated in a reverse phase system.

The separation mechanism of these isomers on the phenyl-bonded phase can be understood from the consideration of dipole-dipole interaction. This

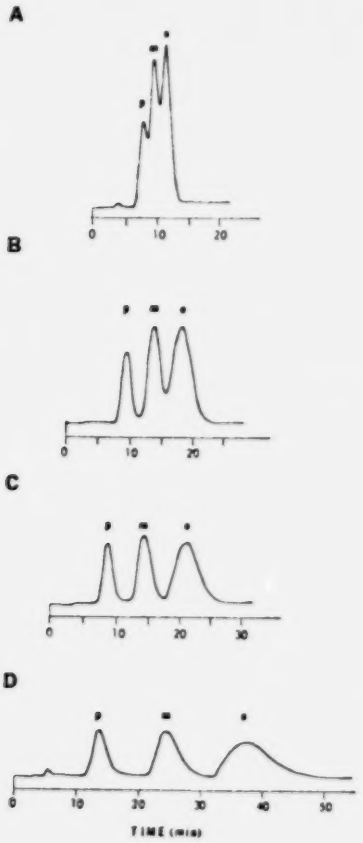

6 Separation of dihydroxybenzene isomers on the phenyl-bonded phase packing at different solvent composition. Column: 60 cm x 0.5 cm i.d., Phenyl Bondpak/Porasil B, 37 ~ 75 μ; temp: ambient; detector: UV (254), 0.1 absorbance, full scale .

(A) 30% methanol/70% water; flow rate: 2 ml/min

(B) 15% methanol/85% water; flow rate: 2 ml/min

(C) 5% methanol/95% water; flow rate: 2.5 ml/min

(D) 0% methanol/100% water; flow rate: 2.5 ml/min

can be proved from the elution order of DNB isomers or DHB isomers. O-DNB, with the strongest dipole moment among three isomers, has the strongest interaction with the dipole developed on the surface of the phenyl-bonded phase. Thus, it was the last species eluted out of the column. M-DNB,which has the second strongest dipole moment,came out second and P-DNB, which has smallest dipole moment,came out first. The same principle is also valid for the separation of DHB isomers. This interaction, however, was not a dominant force on the C_{18} column because of the low polarity of the C_{18} and the residual hydroxyls on the silica. Therefore, a relatively weak dipole-dipole interaction will occur in the C_{18} column, and the change of solvent composition may overcome this force to change the elution order. If this is true, the phenyl-bonded phase should have a better separation for the DHB isomers than the C_{18} column. Besides, the phenyl-bonded phase may have better selectivity for those polar pollutants such as carbamates and nitrosoamines. Most of this work has been published.[9]

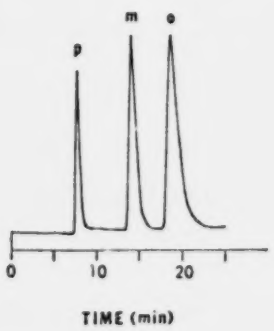

7 Separation of dihydroxybenzene isomers on the octadecyl-bonded phase packing. Column: 30 cm x 0.5 cm i.d., Lichrosorb RP 18, 10μ; temp: ambient; detector: UV (254), 0.1 absorbance, full scale; flow rate: 2 ml/min; solvent composition: 100% water .

COMPARISON OF TWO RECOVERY METHODS ON BONDED PHASE PACKINGS

As mentioned above, both the pumping method and the injection method were used for recovery studies. In the pumping method, a very dilute solution of the solute was passed through the column following which the retained solute was stripped by using a good solvent such as methanol. This is very similar to the procedure that would be followed in the analysis of a real sample. The injection method, however, is a different approach. In this method, a small volume of a concentrated sample was injected into the column followed by a large volume of wash-water prior to stripping with methanol. The second method has the potential advantage of minimizing adsorption losses onto walls of vessels and tubing before the sample enters the column.

The apparatus used for the recovery study is essentially the same as that described above. The column used for this study was the bonded C_{18} packing (20 cm x 0.5 cm). Sevin and naphthalene were the model compounds for these two different methods. The concentration of the sample prepared in methanol was 10^{-3} to 10^{-4} M. In the pumping method, the solution was made by adding a small amount of sample (about 50 μl) to 25 ml of water, then the experiment was carried out according to the following procedure.

(a) Wash the column and the intensifiers with 50 ml MeOH.

(b) Wash the column and the intensifiers with 50 ml H_2O.

(c) Pump the sample solution (25 ml) directly through the column (C_{18}) at a flow rate of 1 ml/min.

(d) Pump 10 ml of clean water through the whole system to clean the sample residue in the intensifiers.

(e) Elute the sample, retained in the column, by using pure MeOH.

The result of this method for Sevin and naphthalene can be seen in Table 2. It is obvious that the measurements obtained from this experiment were not very reproducible and thus no useful data were obtained. The reason for these poor recoveries is adsorption losses as described above. This adsorption problem must definitely be studied further in order to know the exact recovery for a given sample.

In the injection method, the experimental procedure is listed as the following.

(a) Wash the column and the intensifiers with 50 ml MeOH.

(b) Wash the column and the intensifiers with 50 ml H_2O.

(c) Pump water continuously across the column as the mobile phase. Flow rate is adjusted to 1 ml/min.

(d) Inject the sample ($\sim$ 50 μl) into the column.

Table 2. Results of recovery studies on the C_{18} Column using two different methods*

Compound	Pumping Method			
Studied	Trials	Recovery	Trials	Recovery
	1	42%	1	80%
Naphthalene	2	37%	2	87%
	3	10%	3	84%
	4	57%	4	87%
Sevin	1	20%	1	100%
	2	80%	2	100%

*Recovery was measured from the ratio of peak heights

(e) Wash the column with H_2O for 25 minutes or more.

(f) Change the mobile phase to pure MeOH and elute the sample from the column.

The result based on this method is shown in Table 2. It is obvious that these recoveries were very high and reproducible, especially if we compare them with those previously obtained. However, it is important to note that the samples must be soluble in the total amount of washwater. Otherwise, the data are meaningless. It is also obvious from this study that the adsorption losses due to the vessels or tubings are a crucial factor for compound recovery.

Another factor that affects the recovery is the retention volume of the species. If, for example, a species can be eluted from a column using 200 ml of water, such a column cannot be used to preconcentrate that species from 200 ml or more of sample. Although that observation may be obvious when stated in those terms, it appears that low recoveries reported in the literature for some species may have resulted from passing too large a volume of sample through the column used for preconcentration. Phenol, for example, falls into that category.

EFFECT OF A CHANGE IN SOLVENT ON CHROMATOGRAPHIC PEAK SHAPES

Using solutions containing single dihydroxybenzene isomers as well as a solution containing all three, produced an unusual case of peak-splitting. In spite of the fact that water and methanol are completely miscible, each species, when dissolved in alcohol, gave two peaks (or a shoulder plus a peak) when injected into a column and eluted with water. Similarly, an

aqueous sample injected into a methanolic eluent gave the same type of behavior. However, a sample dissolved in water injected into an aqueous eluent or a sample in alcohol injected into an eluent of alcohol gave only a single, sharp peak for each species.

The above observations are important for two reasons. First, care must be exercised in matching solvents if retention times (volumes) of peaks are to be used for identification. Second, column efficiencies can be adversely affected, leading to true overlaps of two different species as a result of peaks for individual species being wider than normal. These results have been published.[10]

COMPARISON OF THE RECOVERY ON TWO DIFFERENT BONDED PHASES

Since two bonded phases were used for the present project, it would be interesting to know which of these two had the better recovery efficiencies for the aromatic compounds tested. At the present time, this study is still not complete; therefore, only preliminary results are available.

The injection method was basically used for both the C_{18} column (20 cm x 0.5 cm) and the phenyl-bonded phase column (30 cm x 0.5 cm). Sevin, matacil, furdan, and naphthalene were tested for the C_{18} column. For the phenyl-bonded phase, 2-naphthol was the only compound used. 2-Naphthol was the only compound commonly used; however, the recoveries of this compound were about the same in these two different systems. It is interesting to note that 2-naphthol and the carbamates (e.g., Sevin, furdan, and matacil) were strongly retained in the C_{18} column even though these compounds are polar. Thus, the C_{18} column may be widely used for different types of compounds. (See Table 3.)

Table 3. Results of recovery studies of some compounds by injection method using two different packings*

Compound	Recovery from the octadecyl-bonded phase packing	Recovery from the phenyl-bonded phase packing
Sevin	90%	
Matacil	83%	
Furdan	93%	
Naphthalene	85%	
2-Naphthol	86%	94%

*Recovery was measured from ratio of peak heights

From the above studies, we know the phenyl-bonded phase has a stronger interaction than C_{18} with some polar compounds (e.g., DNB or DHB). Therefore, the phenyl-bonded phase may be a better column for the concentration and separation of water pollutants like carbamates, herbicides, and nitrosamines. Further study in this area will extend to those nonpolar compounds such as PAH.

SECTION 5

COHERENT ANTI-STOKES RAMAN SPECTROSCOPY

INTRODUCTION TO CARS

There is a rapidly growing need for specific identification systems for liquid chromatography (LC) that can provide a capability comparable to that obtained from the combination of a gas chromatograph with a mass spectrometer. Although attempts have been made to adapt mass spectrometry to liquid chromatography, that marriage is an unrealistic one in the sense that LC can best be used for compounds that are unstable to heat or are non-volatile. In addition to being a specific detector, this technique should be reasonably sensitive and useful with a wide variety of solvents including water.

One technique that would satisfy these requirements is Raman spectroscopy. The major problem with Raman spectroscopy is its inherent inefficiency (1 photon scattered to 10^8 incident). Although resonance Raman spectroscopy allows many orders of magnitude enhancement, this enhancement is often negated by strong fluorescence. Another Raman technique that shows promise is coherent anti-Stokes Raman spectroscopy.

A major goal of our work has been to make a detailed evaluation of coherent anti-Stokes resonance Raman spectroscopy using relatively non-volatile organic compounds, mostly aromatic, that are typical of those encountered in different phases of coal utilization and in the pesticide-insecticide area.

Coherent anti-Stokes Raman spectroscopy (CARS) is a nonlinear optical technique that has been applied to obtain Raman spectra with very high efficiencies[9-22] CARS involves the use of two tunable dye lasers set at frequencies ω_1 and ω_2, respectively. When these two light beams cross in the sample at the phase matching angle Θ, coherent anti-Stokes emission at $\omega_3 = 2\omega_1 - \omega_2$ is generated through the third order nonlinear polarization. This laser-like beam, ω_3, appears on the opposite side of the pump beam, ω_1,

from the Stokes beam ω_2, at the angle Θ. The intensity of the signal is greatly enhanced where the frequency interval, $\omega_1 - \omega_2 = \Delta$, is equal to a Raman active molecular vibrational frequency. Raman spectra are normally obtained by fixing the frequency of ω_1 and varying the frequency of ω_2 and, therefore, changing Δ.

The major drawback to the CARS technique has been the intensity of the background emission resulting from the non-resonant third order susceptibility of the solvent. This usually allows detection limits for solutes of only about 0.05 M. Recently, Chabay, Klauminzer and Hudson[23] have shown that when the ω_1 beam approached an allowed electric dipole transition, the signal generated was greatly enhanced whereas the background emission remained virtually unchanged. This preresonance enhancement allowed the authors to record a very low noise high intensity spectrum of diphenyloclatetraene at concentrations of 1.4×10^{-3} M. By going closer to resonance, this lower limit can be reduced to the micromolar level.

Because CARS starts and ends in the ground state, both energy and momentum must be conserved. For the energy

$$\omega_1 - \omega_2 + \omega_1 - \omega_3 = 0$$

where ω_1 is the pump frequency, ω_2 the stimulating frequency and ω_3 the signal frequency. In this scheme $\omega_3 = 2\omega_1 - \omega_2$. Since the ω_3 signal increases drastically when $\omega_1 - \omega_2 = \omega_r$, the output peaks will occur at $\omega_3 = \omega_1 + \omega_r$ or anti-Stokes shifted. For the momentum

$\overline{P}_1 - \overline{P}_2 + \overline{P}_1 - \overline{P}_3 = 0$ or $2\overline{P}_1 - \overline{P}_2 = \overline{P}_3$

$$P = \frac{h}{\lambda} = \hbar k \text{ or } k = \frac{2\pi}{\lambda} = \frac{2\pi\nu}{c} = \frac{2\pi\nu_o M(\nu_o)}{c}$$

where ν is the frequency in solution and ν_o the frequency in vacuum and $M(\nu_o)$ the index of refraction of the liquid under study. Since the index of refraction varies with frequency (dispersive medium) the vectors $\overline{P}_1$, $\overline{P}_2$ and $\overline{P}_3$ will not lie in a line and

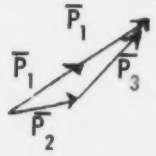

This means that to obtain a signal the beams ω_1 and ω_2 will have to be crossed at an angle Θ. Also, the signal beam, ω_3, will be removed from these beams. Therefore, the CARS technique offers not only higher efficiencies but also essentially complete rejection of fluorescence since the signal beam ω_3 is both spatially and frequency removed from the fluorescence signal. That is, the CARS signal at ω_3 occurs at higher frequency than either of the exciting frequencies. Hence, very efficient (up to 1 in 10^9) discrimination of the natural fluorescence of the molecule is possible because fluorescence involves the emission of energy at lower frequencies than the excitation process. Also, fluorescence occurs over 4π steradians whereas the CARS signal is emitted in a laser-like beam. The fluorescence can be reduced greatly by observing the signal through a pin hole well away from the sample. In our particular setup, the beam passes through an iris 30 cm away from the sample. This corresponds to an f of ~100.

INITIAL SET UP AND SOLVENT STUDIES

In evaluating the applicability of CARS as a specific detector for liquid chromatography, we have had to modify the system to fit our needs. Since each solvent will have a different index of refraction and dispersion, the crossing angle needed to be changed drastically from solvent to solvent. To avoid constant repositioning of the collection optics, a rotation stage was constructed. This stage holds all of the collection optics and detectors and pivots about the crossing point of the ω_1, ω_2, and ω_3 beams. When the crossing angle is changed, the stage is merely rotated to the new angle and all of the optics are in alignment.

Since the dispersion is a function of frequency, the crossing angle and, therefore, the collection stage will need to be varied during the scan. In order to tabulate both crossing angles, and their frequency dependence, the original ω_2 steering mirror was replaced with a vernier drive mirror mount. This mirror allows one to determine a scanning algorithm for computer control of the crossing angle.

SAMPLE CELL DEVELOPMENT

In order to be compatible with high resolution liquid chromatography, the sample cells had to be of small volume (1 to 10μ l). Our preliminary results showed that this prob-

lem could be solved by using standard melting point capillaries. This proved more convenient and considerably less expensive than the standard cuvettes used in past CARS experiments. The capillary was placed in the plane of ω_1 and ω_2 and perpendicular to their bisector. The capillary was then raised or lowered until the ω_1 beam passed undeviated. This placement was critical since the rounded walls greatly displaced the beams unless they travelled along the diameter. This displacement actually made the alignment easier. Once the ω_1 beam passed undeviated, the steering mirror for the ω_2 beam was adjusted to make it pass undeviated. This visual alignment is much more sensitive than the knife edge test for vertical placement. Once aligned vertically, the steering mirror for the ω_2 beam was adjusted horizontally to obtain the CARS signal. The loss in signal compared to a cuvette is only on the order of 10%.

In order to test the feasibility of observing CARS signals in a flowing system, we have simulated the flow conditions experienced in a liquid chromatograph by using an infusion pump. Even at maximum flow rates, no additional noise was observed. Based on the cylindrical shape and inside diameter (1.2 mm) we have calculated and experimentally verified that flow rates as high as two meters per second can be used without turbulent flow disturbing the beams.

SIGNAL ENHANCEMENT IN THE RIGOROUS RESONANCE REGION

Studies of the CARS intensity as a function of excitation wavelength had not been previously made in the rigorous resonance region. We have attempted to compare the experimental resonance profiles with those calculated using the Albrecht theory[24,25] modified for CARS by Hudson et al.[26] β-Carotene was chosen as a model system because of the extensive work carried out by Miyazawa and coworkers[27] on the excitation profiles for the spontaneous Raman effect. The parameters derived by these workers were directly transferable for our experiment.

A portion of the CARS spectrum of β-carotene in benzene solution is shown in Figure 8. The pump frequency used, 575 nm, is in the preresonance region. The spectrum observed compares favorably in both frequency and relative intensity with that reported by Rimai et al.[28] The weak peaks at 1193 and 1215 cm^{-1} reported in this reference are evident in Figure 8.

Since Miyazawa and coworkers[27] found that ν_1, at 1527 cm^{-1}, the CC double bond stretching mode, and ν_2, at 1158 cm^{-1}, the CC single bond stretching mode, accounted quite well for the electronic absorption progression in the region between 400–500 nm, we chose to study the coherent anti-Stokes Raman excitation profiles for these two lines.

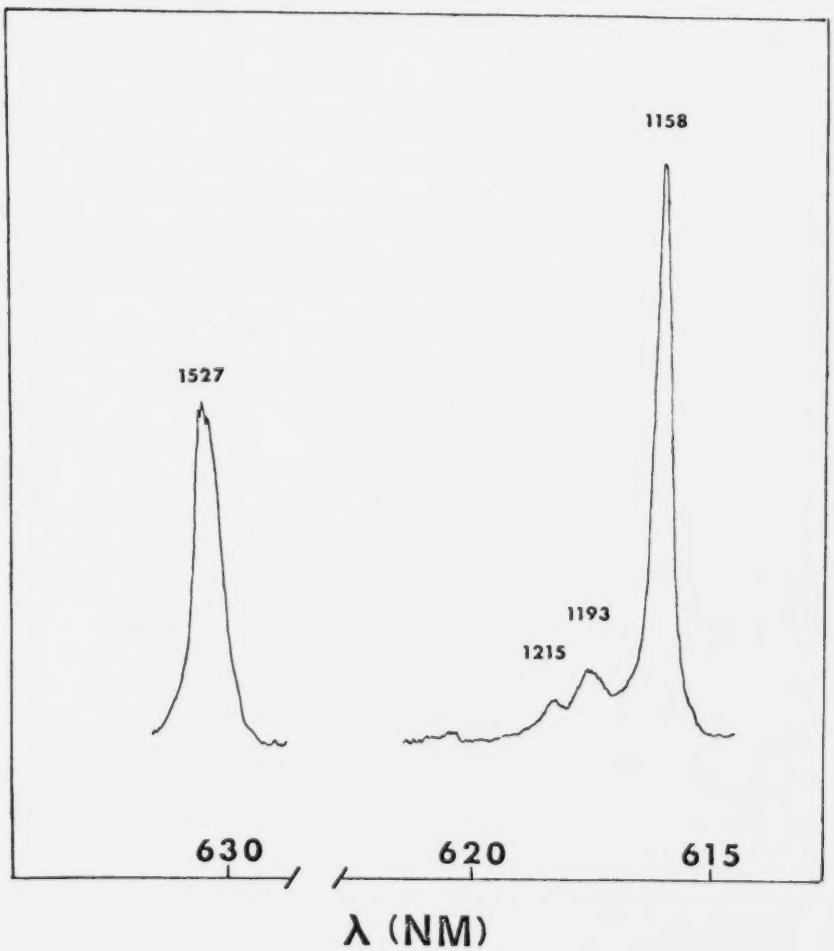

8 A portion of the preresonance coherent anti-Stokes Raman spectrum of trans-beta-carotene. ω_1 is 575 nm. The concentration is 10^{-3} M.

The intensity of a CARS signal is proportional to the square of the third order susceptibility. This susceptibility is the sum of two terms,

$$\chi^{(3)} = \chi^{(3)}_E + \chi^{(3)}_R \tag{1}$$

where $\chi^{(3)}_E$ is the electronic susceptibility and $\chi^{(3)}_R$ is the Raman susceptibility. $\chi^{(3)}_E$ is a slowly varying function of the frequency difference $\omega_1 - \omega_2 = \Delta$ and the sum is dominated by the Raman susceptibility when Δ is equal to an allowed Raman frequency ($\Delta = \omega_r$) of the molecule. As shown by Hudson et al.[18] when $\Delta = \omega_r$ $\chi^{(3)}_R$ is given by

$$\chi^{(3)}_R \doteq \left(\frac{N \pi C^4}{i h \omega_1 \omega_2^3 \Gamma_r}\right) a^*(\omega_1)\, a(\omega_3) \tag{2}$$

where N is the number density and Γ_r the Raman linewidth. The treatment of the spontaneous resonance Raman data for β-carotene by Miyazawa et al. followed the development of Tang and Albrecht. The expression for the scattering tensor, a, is given by

$$\left(a_{\sigma\rho}^{(\omega_1)}\right)_{ij} = A + B \tag{3}$$

where

$$A = \sum_{b \neq g}{}' \sum_{v} \left(\frac{\langle g|R_\sigma|b\rangle\langle b|R_\rho|g\rangle}{\omega_{bv} - \omega_1 + i\Gamma_b} + \frac{\langle g|R_\rho|b\rangle\langle b|R_\sigma|g\rangle}{\omega_{bv} + \omega_2 + i\Gamma_b} \right) \langle i|v\rangle\langle v|j\rangle \tag{4}$$

$$B = \sum_{b \neq g}{}' \sum_{v} \sum_{a \neq b} \sum_{q} \left[\left\{ \frac{\langle g|R_\sigma|b\rangle\langle b|h_q|a\rangle\langle a|R_\rho|g\rangle}{\omega_{bv} - \omega_1 + i\Gamma_b} + \frac{\langle g|R_\rho|b\rangle\langle b|h_q|a\rangle\langle |R_\sigma|g\rangle}{\omega_{bv} + \omega_2 + i\Gamma_b} \right. \right.$$

$$\chi \langle i | v \rangle \langle v | Q_q | j \rangle / (\omega_{bo} - \omega_{ao}) \qquad (5)$$

$$+ \left\{ \frac{\langle g | R_\sigma | a \rangle \langle a | h_q | b \rangle \langle b | R_\rho | g \rangle}{\omega_{bv} - \omega_1 + i\Gamma_b} \right.$$

$$\left. + \frac{\langle g | R_\rho | a \rangle \langle a | h_q | b \rangle \langle b | R_\sigma | g \rangle}{\omega_{bv} + \omega_2 + i\Gamma_b} \right\} \chi$$

$$\langle i | Q_q | v \rangle \langle v | i \rangle / \omega_{bo} - \omega_{ao}$$

where the terms are identified as follows.

g	=	ground electronic state
i, j	=	vibrational states in the ground electronic states
a, b	=	excited electronic states
v	=	vibrational state in the excited electronic state
ρ, σ	=	x, y or z
R_σ	=	σ th component of the electric dipole moment operator
h_q	=	vibronic coupling operator $\delta H / \delta Q_q$ with H = electronic Hamiltonian
Q_q	=	q'th normal coordinate of the ground electronic state
Γ_b	=	halfwidth of the g → b electronic transition

Miyazawa et al., determined that the contribution of the B term was negligible for the symmetric modes, ν_1 and ν_2, in the rigorous resonance region. They calculated the separations between the equilibrium positions of the ground and electronic excited states for the ν_1 and ν_2 modes by treating these as adjustable parameters to fit the experimental excitation profiles. These values then reproduced the observed low temperature absorption spectrum when a Lorentzian halfwidth of 250 cm^{-1} was used for the electronic absorption lines.

In order to calculate the theoretical CARS excitation profiles, we have used the separation parameters of Miyazawa et al. and have increased the electronic halfwidth Γ_b, to 500 cm^{-1} since our measurements were made at room temperature[21]. This halfwidth reproduced the electronic absorption spectrum at room temperature. The separation parameters used were 1.1 for ν_1, and 1.4 for ν_2 corresponding to an elongation of 0.02Å for the C = C bonds and contraction of -0.031Å for the C - C bonds. The frequencies in the ground and excited states were assumed to be equal and the summation over v was taken to v = 8. Using this procedure, we have calculated relative values of $|\chi_R^{(3)}|^2$ and these are the solid curves shown in Figures 9 and 10. For comparison, we have calculated the excitation profiles for the spontaneous Raman effect for the same experimental conditions. These are shown in Figure 11 and 12. By comparing Figures 9 with 11 and 10 with 12 it is evident that there is a significant difference between the CARS and spontaneous Raman excitation profiles.

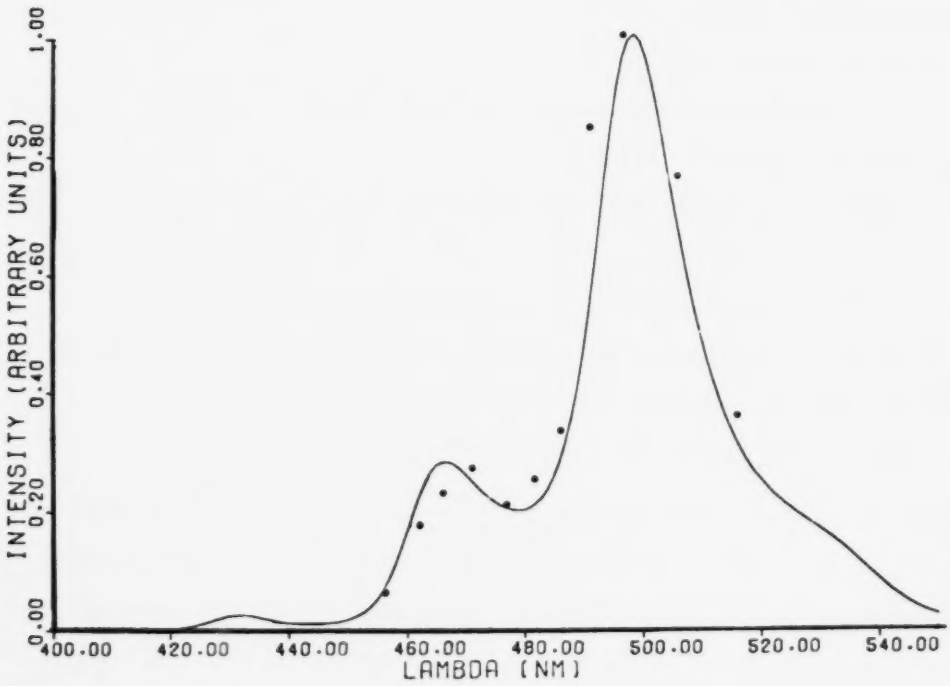

9 Observed (...) and calculated (solid line) CARS excitation profile for the ν_1 vibrational mode of beta-carotene .

Several of the CARS experimental points were obtainable with different sets of dyes. In particular, the point at 570 nm could be done using coumarin dyes 485 and 495 or coumarin dyes 500 and 485. When first attempting these experiments, we noted serious discrepancies between the ratio of the intensity of ν_2 to the benzene 992 cm^{-1} line depending on which set of dyes were used. The major difference in the two experiments was the power in ω_1. Since the CARS signal of both the solute and solvent lines should vary with the square of the power in ω_1 and linearly with the power in ω_2, this ratio should have remained constant. A plot of log $P\omega_3$ vs log $P\omega_1$ should be linear with slope 2. Figure 13 indicates that the solvent signal (992 cm^{-1} benzene line) does have slope 2 over a wide power range in ω_1. At very low powers, the solute signal (ν_2 1158 cm^{-1}) did follow the expected slope 2 curve. However, it deviated markedly from this line at higher powers. In fact, at very high powers, the signal was lost in the background emission. This explains the anomalous results obtained at 510 nm with the two sets of dyes.

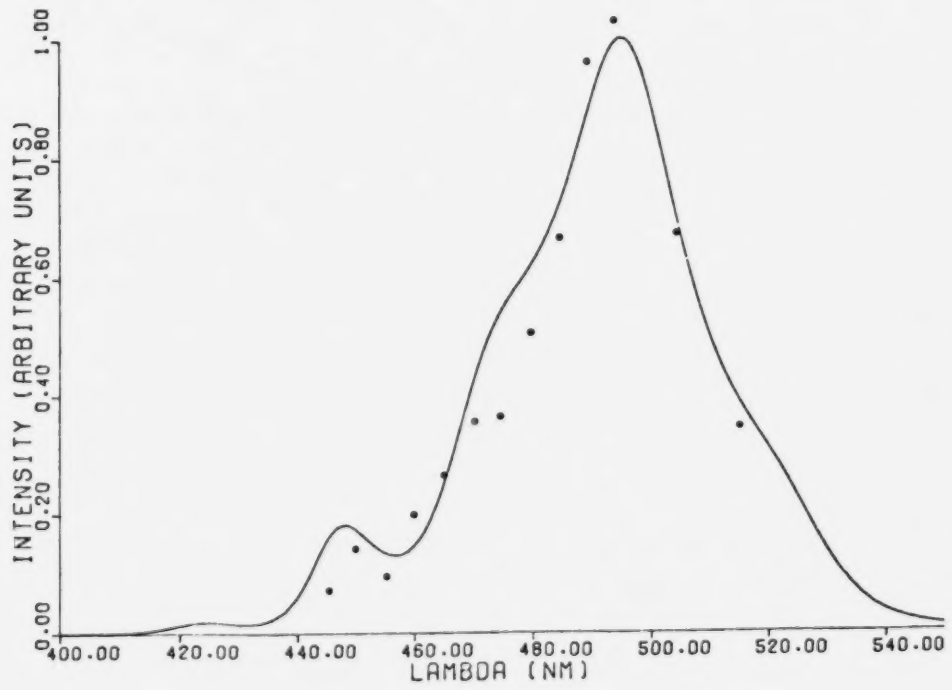

10 Observed (...) and calculated (solid line) CARS excitation profile for the ν_2 vibrational mode of beta-carotene .

The solution to this problem was to lower the laser power in ω_1, 1) by using the nitrogen laser at lower power, 2) by attenuating ω_1 by the use of neutral density filters. This resulted in peak powers in ω_1 of ~1 kW.

It is possible to gain some insight into the cause of this phenomenon by considering a simple calculation. At a power of ~100 kW in ω_1 with a coherence length of ~1 mm, there will be $\sim 10^{15}$ photons/ pulse (pulse length ~6 to 8 nsec) passing through the focal volume. In this volume at 10^{-4} M, there are $\sim 10^{11}$ solute molecules. Since the decadic molar extinction coefficient of β- carotene is $\sim 10^{5}$ liter $mole^{-1}$ cm^{-1}, it is quite possible that the system saturates, and increasing the intensity of ω_1 has no effect on the solute CARS signal but only increases the background. Assuming ω_1 is intense enough to saturate and steady state populations of the vibrational levels of the ground electronic state result, then the intensity of ω_3 is independent of ω_1. It may be that the power of ω_3 for β-carotene is asymptotically approaching a limit (Figure 13).

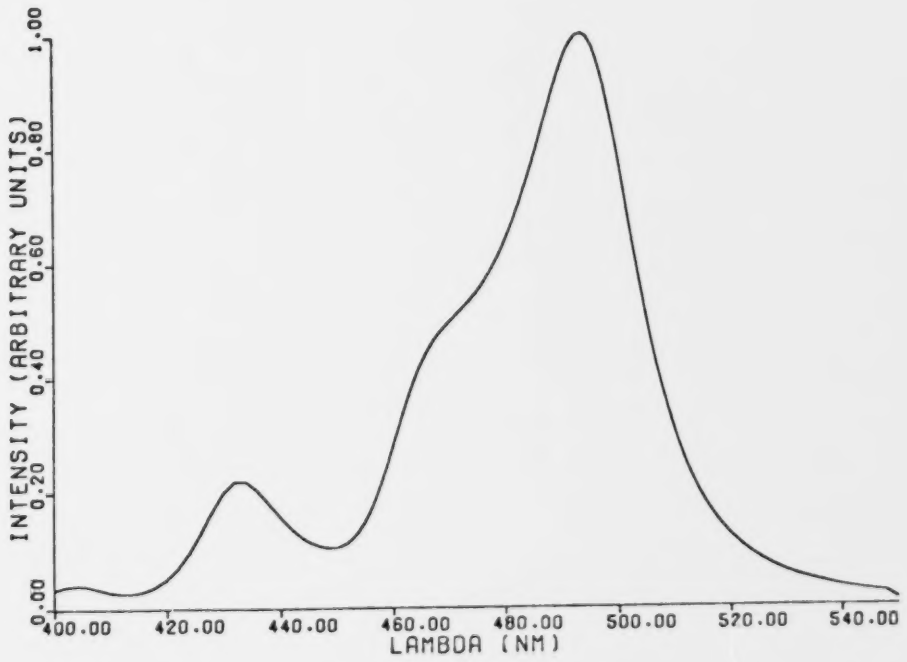

11 Calculated spontaneous Raman excitation profile for the ν_1 vibration of beta-carotene using the same parameters as in Figure 3 .

Once we discovered the necessity of lowering the laser power, it was possible to determine when we were operating in the linear region. β-carotene lines to the benzene 992 cm^{-1} line and continuing to lower the power in ω_1 until no change in the ratio resulted. We had already switched to photomultiplier detection for experiments at low power in the UV region using frequency doubling. Due to the low power required in the resonance experiments reported here, ~1 kW peak power, photomultiplier detection was also essential. Once at low power, the determination of the excitation profiles proceeded rapidly.

The ratios of the intensity of β-carotene lines to the benzene 992 cm^{-1} line were corrected for the power differences and absorption differences at the various wavelengths. This corrected ratio for ν_i i = 1, 2 is given by

$$R_i = \frac{P_{\omega 3}(\nu_i)}{P_{\omega 3}(\phi)} \cdot \frac{P^{o}_{\omega 2}(\phi)}{P^{o}_{\omega 2}(\nu_i)} \cdot \frac{10^{A_{\omega 2}(\nu_i)}}{10^{A_{\omega}(\phi)}} \cdot \frac{10^{A_{\omega 3}(\nu_i)}}{10^{A_{\omega 3}(\phi)}} \qquad (6)$$

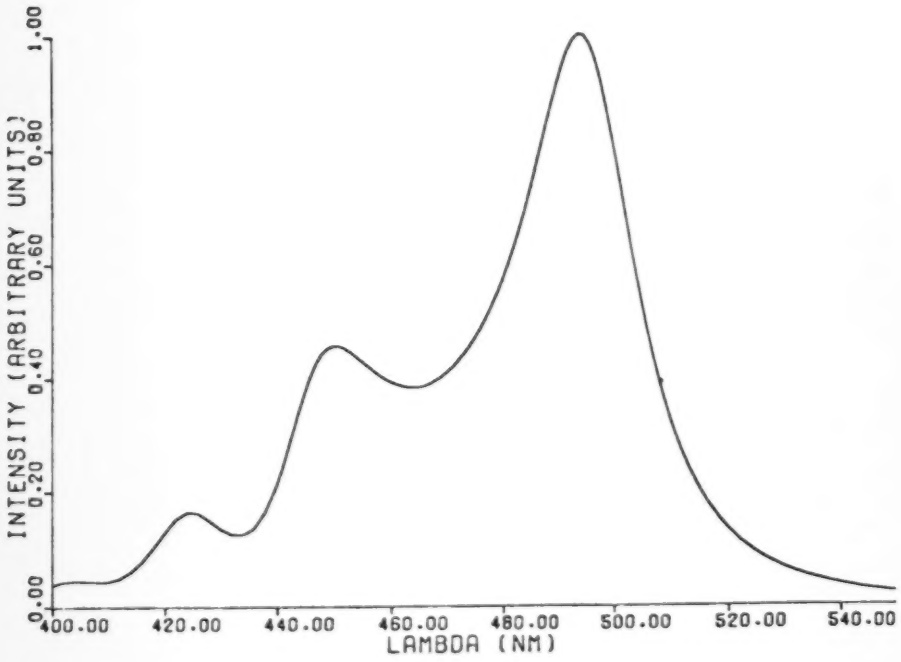

12 Calculated spontaneous Raman excitation profile for the ν_2 vibration of beta-carotene using the same parameters as in Figure 4 .

where

$P_{\omega}(\nu_i)$ is the observed power at frequency ω for the β - carotene

$P_{\omega}(\phi)$ is the observed power at frequency ω for benzene

$A_{\omega}(\nu_i)$ is the absorbance at ω for β - carotene

$A_{\omega}(\phi)$ is the absorbance at ω for benzene.

Since $P^{o}_{\omega 2} = P_{\omega 2} 10^{A_{\omega 2}}$ Eq. (6) reduces to

$$R_i = \frac{P_{\omega 3}(\nu_i)}{P_{\omega 3}(\phi)} \cdot \frac{P_{\omega 2}(\phi)}{P_{\omega 2}(\nu_i)} \cdot \frac{10^{A_{\omega 3}(\nu_i)}}{10^{A_{\omega 3}(\phi)}}$$

where $P_{\omega 2}$ is the power measured in ω_2 after passing through the sample. This also proved

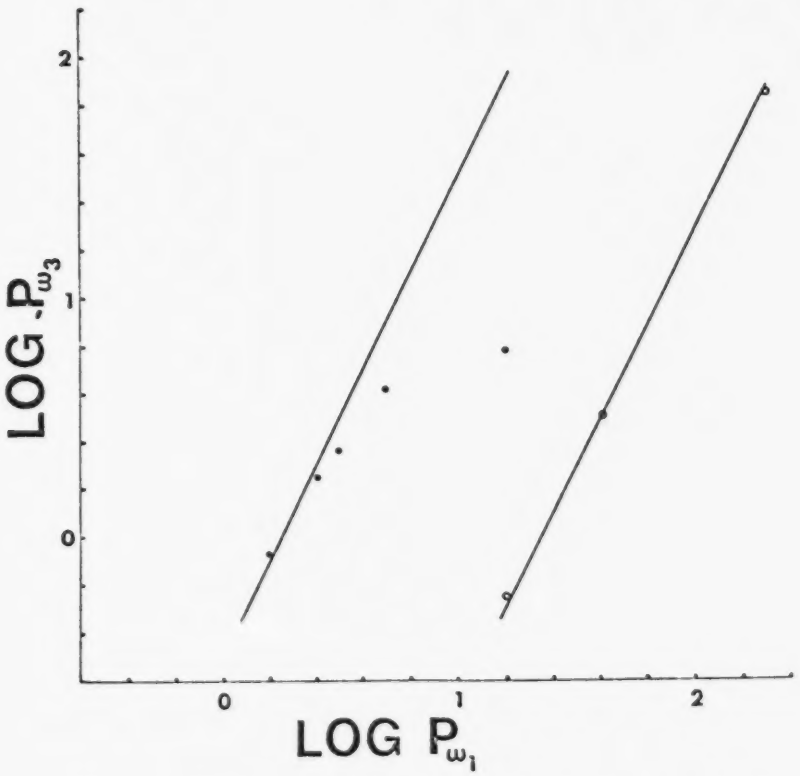

13 Plot of the log of the power in ω_1 versus the log of the power in ω_3 for trans-beta-carotene (·) and benzene (O).

to be a very convenient method since it was possible to determine the ratio $P_{\omega 2}(\phi)/P_{\omega 2}(\nu_1)$ simply by measuring the relative powers at the three frequencies without the necessity of moving the sample. It was, however, absolutely necessary to adjust the crossing angle to maximize the signal at each of the three frequencies (i.e. ν_1, ν_2 and ν_ϕ) in order to obtain reliable ratios. The experimental points for ν_1 and ν_2 are indicated in Figures 9 and 10. The agreement between the experimental points and the curves generated using the known parameters determined from the spontaneous resonance Raman effect is quite reasonable.

These experiments show that the CARS technique is applicable to the determination of excitation profiles. Since the method is also fluorescence rejecting, it may be applied to molecules whose fluorescence prohibits the observation of spontaneous resonance Raman profiles. We have shown that resonance CARS experiments may be performed with con-considerably lower power laser systems than the system used here. If,however, one wishes to extend these experiments to wavelengths shorter than 360 nm, in which inherently inefficient frequency doubling must be used, then high power lasers are necessary. This extension is desirable because of the much wider range of molecular systems accessible to resonance experiments.

With the program developed and the UV-visible absorption spectrum, it will be possible to predict the pump frequencies which will give optimum signal generation. For our model system this allowed us to detect concentrations of 5 to 7×10^{-7} M. Since this CARS setup can be used with cells of 1 µl volume, we can easily detect 1-2 nanograms of sample.

PHOTOMULTIPLIER DETECTION

For reasons mentioned above, it was necessary to use low laser power in order to obtain meaningful results. This was accomplished by the use of neutral density filters in the ω_1 beam and/or by lowering the power of the nitrogen pump laser. The resultant decrease in signal strength was more than compensated by changing from pin diode to photomultiplier detection. So as to be compatible with the wide wavelength range available using nitrogen laser pumped dye lasers (260 to 740nm) we have used an RCA

C31034 gallium arsenide photomultiplier tube having ~10% quantum efficiency throughout this range. Since target size of this tube is fairly large (4 x 10 mm), the image-object movement was negligible.

RAMAN SPECTRA OF FLUORESCENT COMPOUNDS

The real advantage of resonance enhanced coherent anti-Stokes Raman spectroscopy over spontaneous resonance Raman spectroscopy is its ability to reject fluorescence. We have observed resonance enhancement in several fluorescent compounds whose spectra (even in preresonance) are partially or totally obscured by background fluorescence. Figure 14 shows a pre-resonance enhanced spectrum of β-carboline. This compound shows annoying fluorescence even when irradiated in the yellow and red portions of the spectrum. Another spectrum which is particularly difficult to obtain using the spontaneous

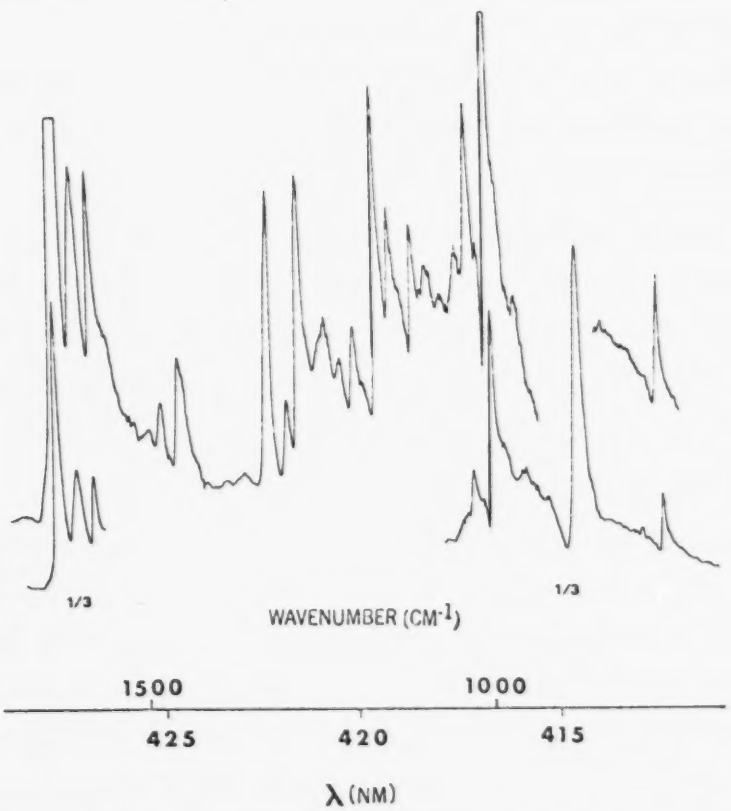

14 Preresonance CARS spectrum of beta-carboline.

Raman effect is β-naphthol. The spectrum shown in Figure 15 was recorded using a pump frequency of 365 nm--a region too highly fluorescing to obtain a spontaneous Raman spectrum.

UV EXPERIMENTS

In order to obtain maximum detection sensitivity for most aromatic compounds, it will be necessary to pump their $\pi - \pi^*$ transitions in the UV. To work in this region (below 360 nm) it is necessary to frequency double the visible output of the dye lasers. Since this is a relatively inefficient process (~10% conversion), we expect to lose about 10^3 in signal strength. This loss is more than compensated by switching to photomultiplier (PM) detection. PM detection is $\sim 10^6$ more times sensitive than conventional pin diode detection. By switching to PM detection and using fused silica optics, we have been able to record the first CARS spectra recorded in the UV region. The lines

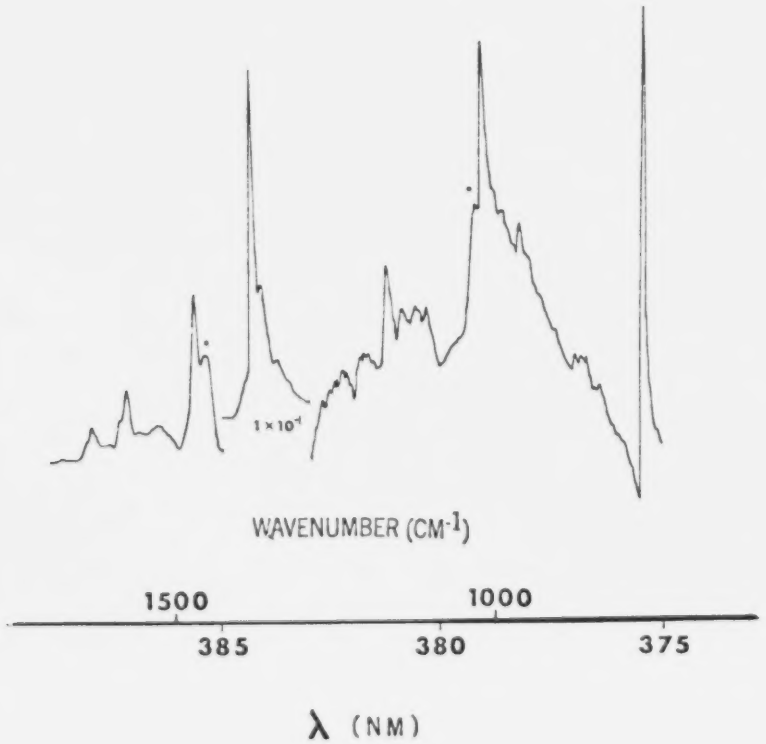

15 Preresonance CARS spectrum of beta-naphthol.

in the CH stretch region of CH_3OH are shown in Figure 16. A complete automated CARS scan in the UV region is shown in Figure 17.

LINESHAPES IN CARS SPECTRA

Under certain conditions, when the laser pump frequency approaches an electronic transition frequency, negative peaks have been observed in coherent anti-Stokes Raman spectra. Two conflicting explanations of this phenomenon have been offered. We have noted that these two explanations lead to a different dependence of the intensity of the negative peaks on the power in the pump beam. We have experimentally determined this power dependence in the case of a 5×10^{-3} M solution of

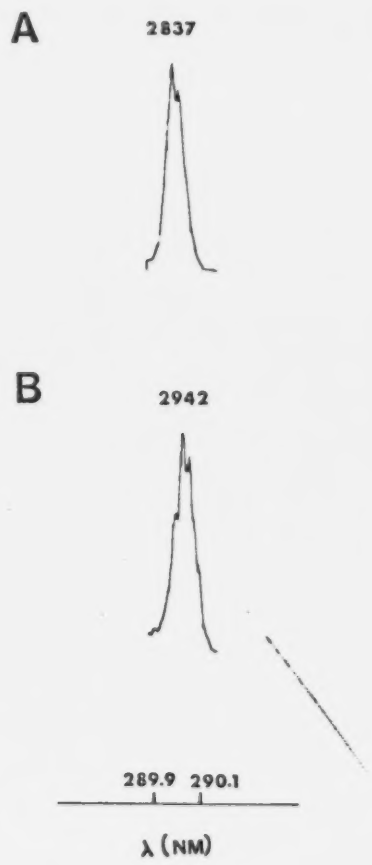

16 UV-CARS spectrum of the CH stretch region in methanol.

N, N-diethyl-p-nitrosoaniline in benzene and found that the intensity of the negative peaks varies with the square of the power in the pump beam. This result is consistent with the explanation that the negative peaks arise from a cross term between the background susceptibility and the imaginary part of the Raman susceptibility and not from the Inverse Raman Effect.

PRERESONANCE ENHANCEMENT OF FLUORESCENT COMPOUNDS

In order for CARS to be a totally versatile technique, the CARS spectra of fluorescent compounds must be able to be resonance enhanced in the presence of strong background fluorescence. In order to show that CARS is a versatile technique, we have undertaken the investigation of the preresonance excitation profiles of the fluorescent compounds β-naphthol and the β-naphtholate ion. The fluorescence rejection of the CARS

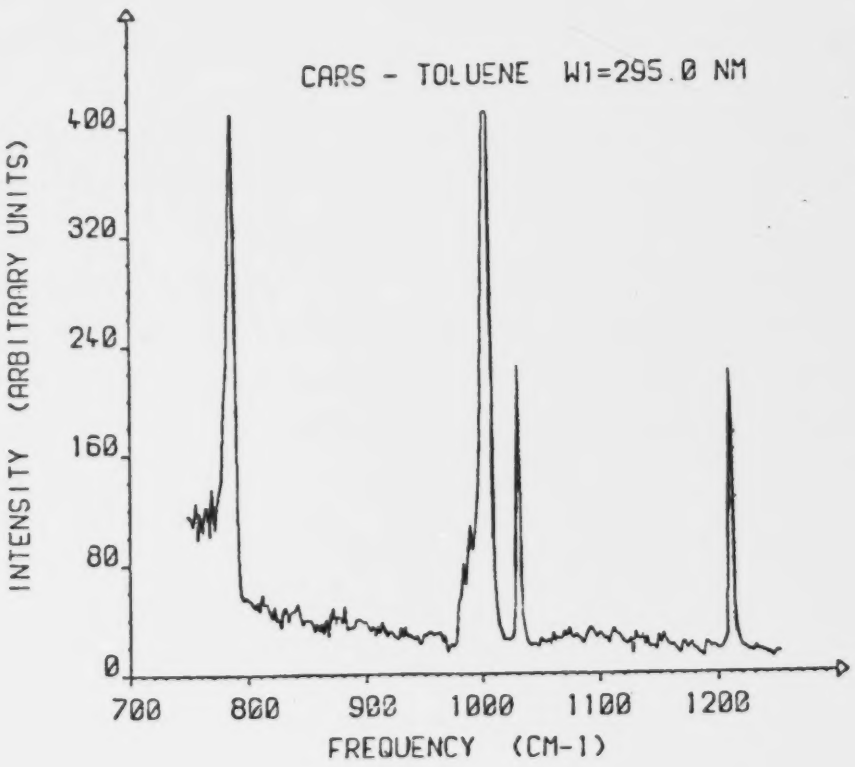

17 Automated UV-CARS spectrum of toluene .

technique allowed Raman spectra to be obtained in a region where fluorescence would obscure the spontaneous Raman signal. A method of taking the ratio of the Raman resonant CARS signal to the background signal allowed for a more convenient and reliable method of generating CARS excitation profiles. The observed excitation profiles are in excellent agreement with those predicted using a single line approximation.

RESONANCE ENHANCEMENT OF FLUORESCENT COMPOUNDS NEAR THEIR ABSORPTION MAXIMUM

In these studies, we have investigated the resonance enhancement of highly fluorescent compounds near their absorption maxima. An empirical rule for determining the minimum detectable concentration has been found to be given by $C_{min} = (10 \cdot E)^{-1}$ where E is the decadic molar absorption coefficient. For most compounds studied thus far, C_{min} falls between 10^{-5} M and 10^{-6} M, well within the range necessary for CARS to be useful for providing specific structural information on liquid chromatographic eluents.

The CARS spectra of several of the compounds are shown in Figures 18 to 23. These spectra have been recorded using concentrations ranging from 1×10^{-5} M to 7×10^{-5} M.

We have conducted an in-depth excitation profile study for the polyaromatic hydrocarbon tetracene (naphthacene). The experimental results agree extremely well with those predicted using CARS resonance theory . The comparison of the experimental results and theory is given in Figure 24.

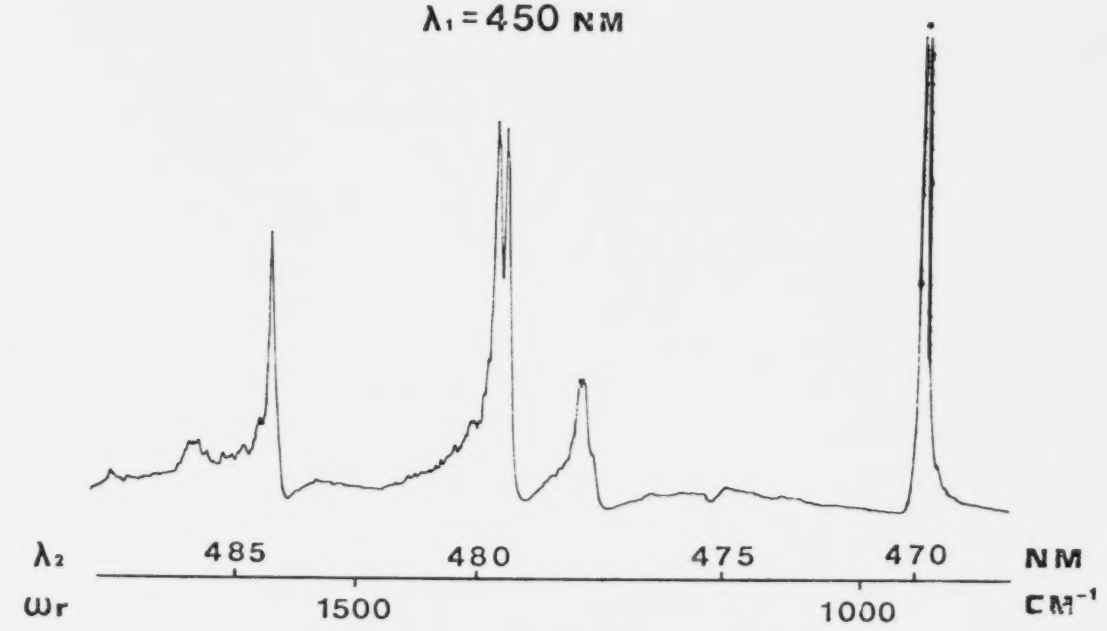

18 CARS spectrum of perylene in benzene taken at a pump wavelength of 450 nm. The quantum efficiency of fluorescence for this compound is .94

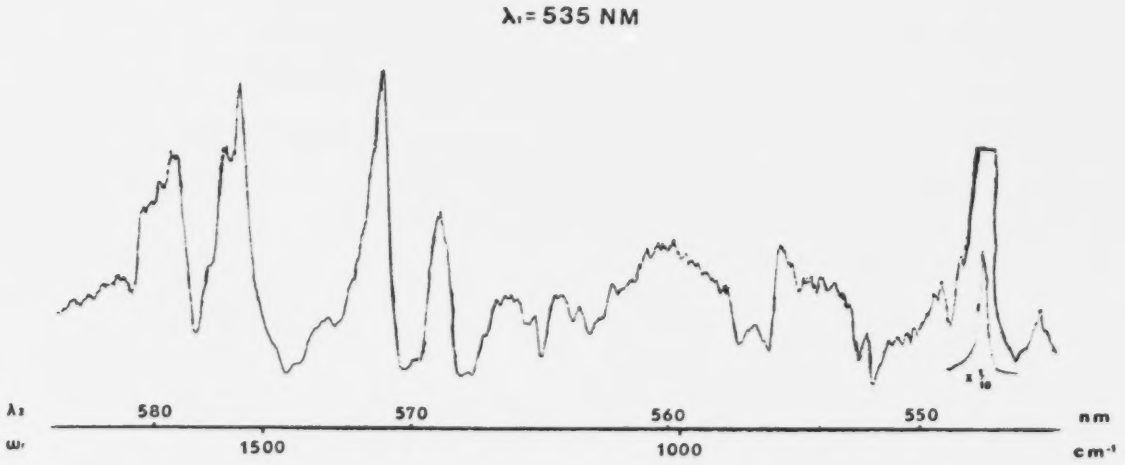

19 CARS spectrum of rhodamine 6G in ethanol taken at a pump wavelength of 535 nm. The quantum efficiency of fluorescence for this compound in ethanol is .95

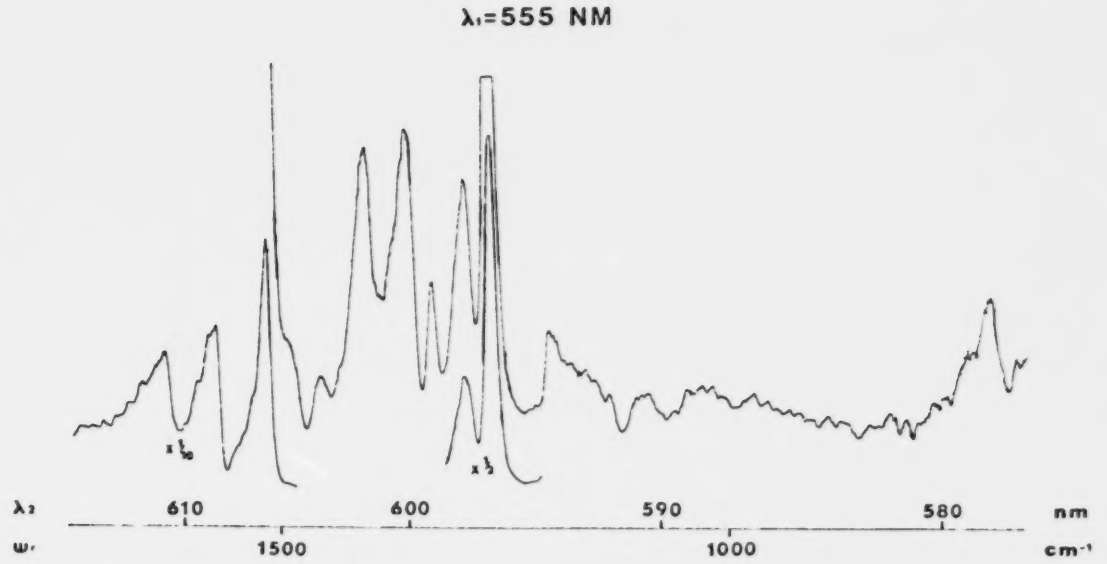

20 CARS spectrum of rhodamine B in ethanol taken at a pump wavelength of 555 nm. The quantum efficiency of fluorescence for this compound in ethanol is .40.

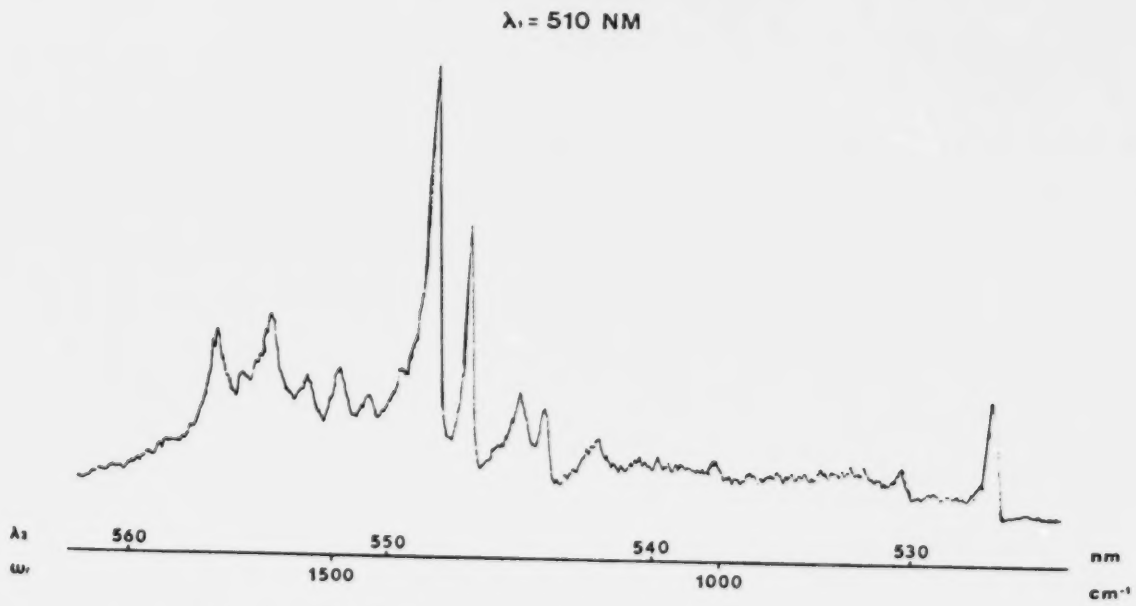

21 CARS spectrum of sodium fluorescein in water at an alkaline pH taken at a pump wavelength of 510 nm. The quantum efficiency of fluorescence for this compound is .90.

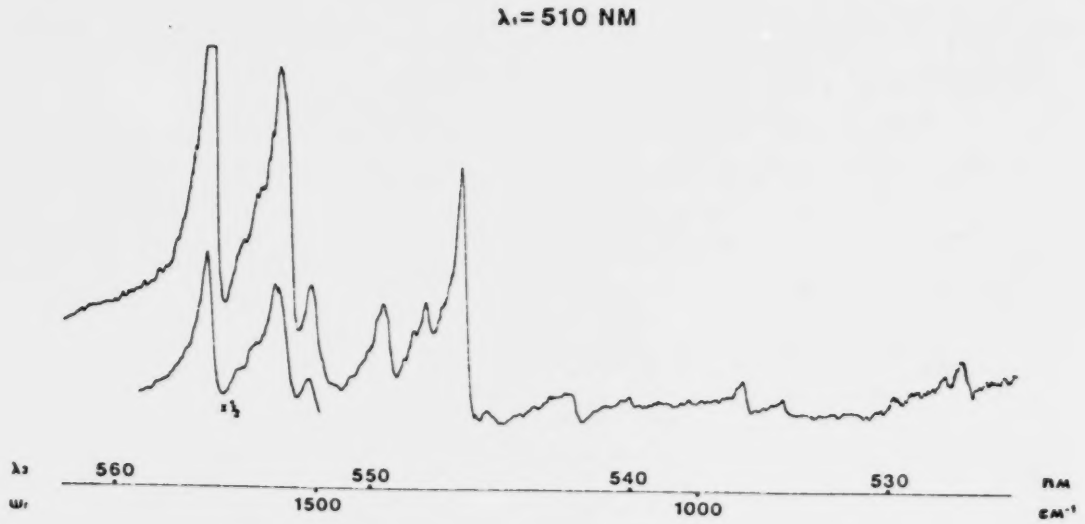

22 CARS spectrum of acridine orange in water at a pump wavelength of 510 nm. The quantum efficiency of fluorescence for this compound is above .50.

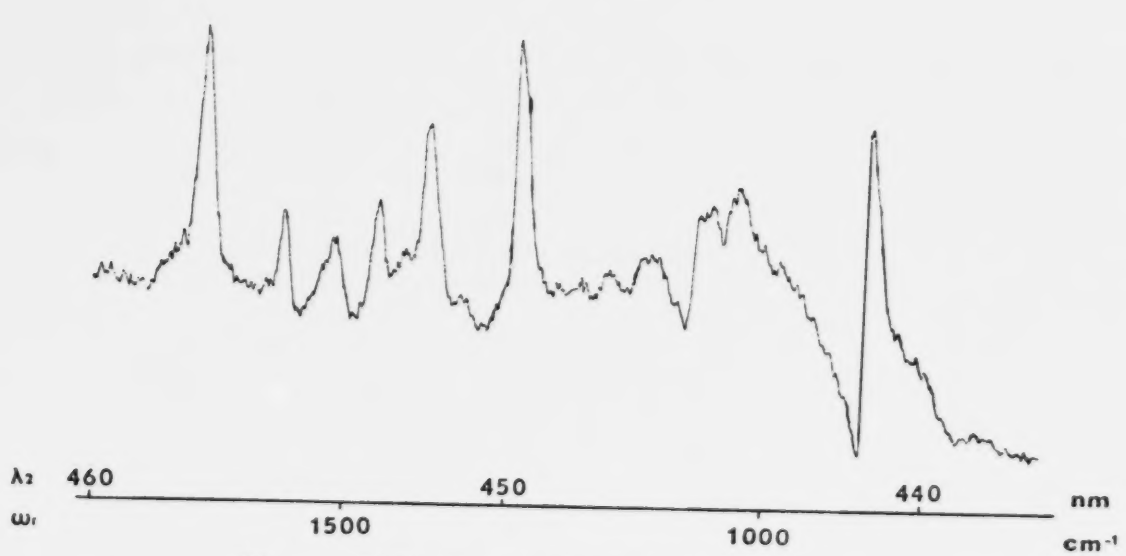

23 CARS spectrum of coumarin 495 in ethanol at a pump wavelength of 425 nm. The quantum efficiency of fluorescence for this compound is above .70.

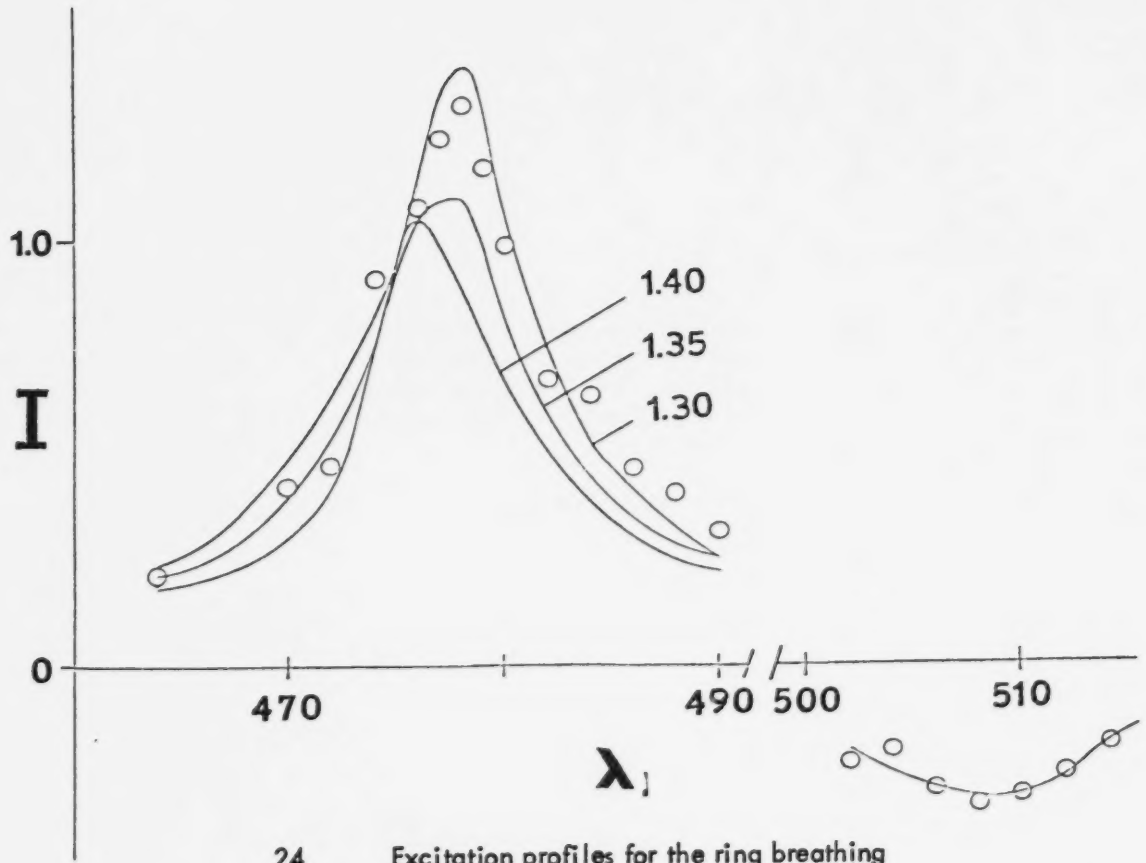

24 Excitation profiles for the ring breathing mode of tetracene as a function of the pump wavelength and displacement parameter. The solid lines represent the theoretical profile at various displacement parameters. The circles represent the experimentally obtained values.

SECTION 6
COMPUTER INTERFACE

The CARS experiment is a multi-parameter process that requires precise control of mirror and micrometer movements. To obtain large frequency scans in short periods of time, it is necessary to control the various parameters by a computer. The minicomputer chosen for this purpose was a PDP 11/34 with such options as dual floppy disk, two general purpose I/O ports (DR11K and DR11C), analog to digital converter (AD11K) with multiplexer (AM11K), and digital to analog converter (AA11K). Included with this package was Digital's RT-11 realtime FORTRAN software package for real time control.

Figure 25 shows the CARS setup employed for these experiments. It consists of a nitrogen laser split into two beams by a 2:1 beam splitter. These beams are then used to pump two Molectron DL200 dye lasers that create the pump (ω_1) and probe (ω_2) beam for the CARS experiment. Scanning of the dye lasers is achieved by a sine-bar-driven grating. The ω_2 dye laser came equipped with a stepping motor drive for continuous scanning. The controller for this dye laser stepping motor is Molectron's DL-040A scan control unit. The two beams are crossed and focused in the sample by lens 2. A Raman signal results when the difference in frequency of the two lasers differ by an allowed Raman transition. The resulting CARS signal (ω_3) is generated at an angle Θ' with respect to the $\omega_1$beam.

In order to detect this signal the detector and monochromator network had to be able to follow the Θ' angle as the scan was taken. This was accomplished by mounting them on a movable stage pivoted about the crossing point of the pump and probe beams. This stage allows the angle of collection to be varied synchronously with the crossing angle. The signal beam, ω_3, passes through an iris 30cm from the sample. The beam is then focused onto the entrance slits of the monochromator network consisting of two Jobin-Yvon model HR10 units mounted front to back. The signals from the photomultiplier and the reference detector (Molectron LP-141) are fed to a Molectron LP-20 boxcar integrator-ratiometer and sent to a analog to digital converter where it is stored and processed by a PDP-11/34 minicomputer.

Computer control of the CARS experiment required the incorporation of a minimum of five stepping motors. Three were required for variation of the cross angle. They controlled mirror translation, vertical and horizontal rotation. The horizontal and vertical rotation stepping motors were 400 steps/revolution while all other motors employed were 200 step/revolution. The collection stage position as well as the monochromator scanning also had to be controlled by stepping motors.

Three types of interfaces had to be built in order to make the CARS unit compatible with the minicomputer. They were: A) busing system for the I/O ports (peribus), B) DL-040A Molectron scan unit interface, and C) stepping motor interfaces.

The design was from the modular concept developed at Purdue[29] . The peribus (peripheral bus) was constructed to increase the number of possible I/O ports. This is achieved by busing all of the bits from the DRII port to a network of plug-in ports. This allows more devices to have access to the same I/O interface. In order for the

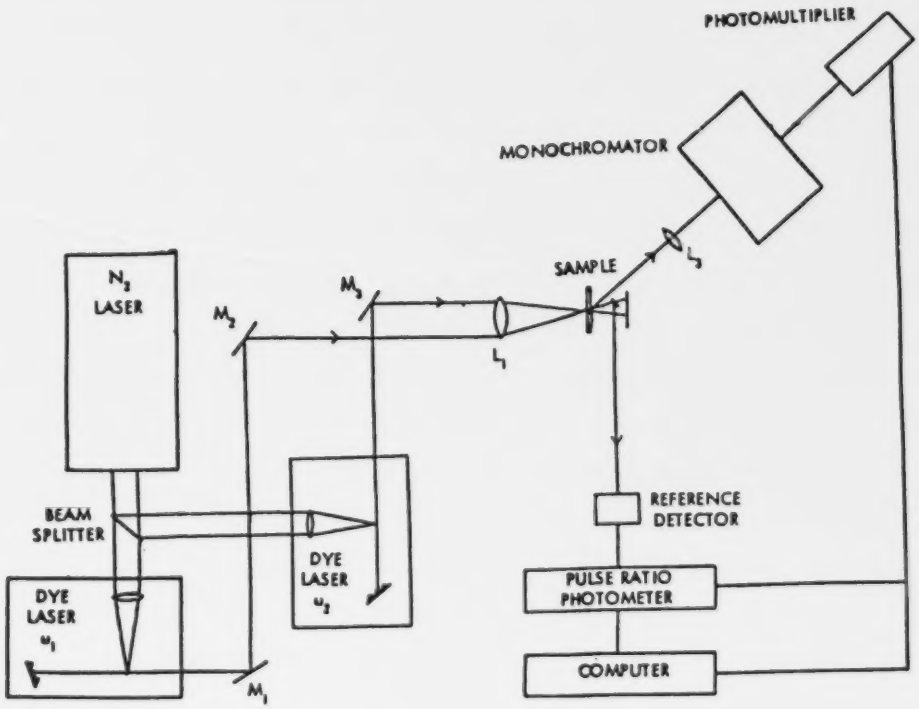

25 Experimental CARS setup used in the studies.

computer to determine which device was being controlled by the I/O interface, each device or operation had to have its own address. If one uses 6-bits of the output word (16-bits) for addressing the various instrumental functions, there are 64 possible addresses and thus operations which can be controlled by a single I/O interface. Figure 26 shows the schematic for the peribus system. It consists of open collector drivers which boost

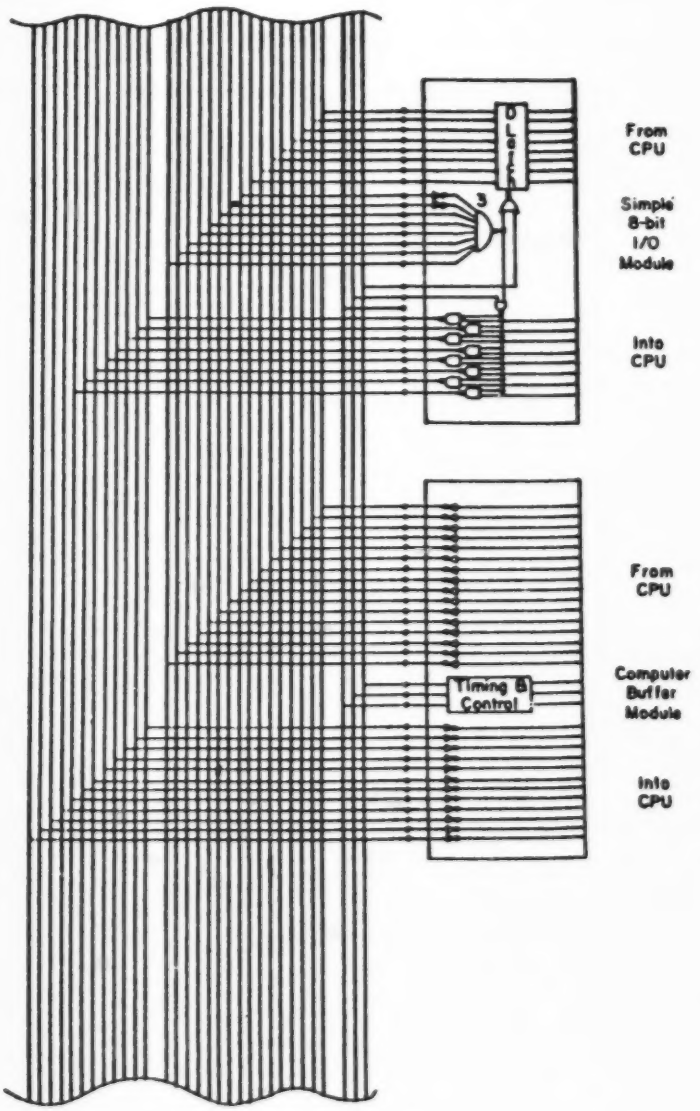

26 Schematic of the peripheral bus.

and distribute the signal from the DR11 I/O port to the various interfaces. It also contains a monostable multivibrator for lengthening various pulses (such as the data-available pulse) put out by the computer. The data available pulse is lengthened to 4μ sec by the peribus and used in the address decode. By doing this, the information of the output word is insured of being valid.

The scan unit has three types of operations that had to be interfaced to the computer. They included data input (latching), data output and pulse generation. A simplified scheme of how these operations are handled is shown in Figure 27. The operations that required latching were those in which a level (high or low) had to be held for long periods of time. Data output was accomplished by two input open collector

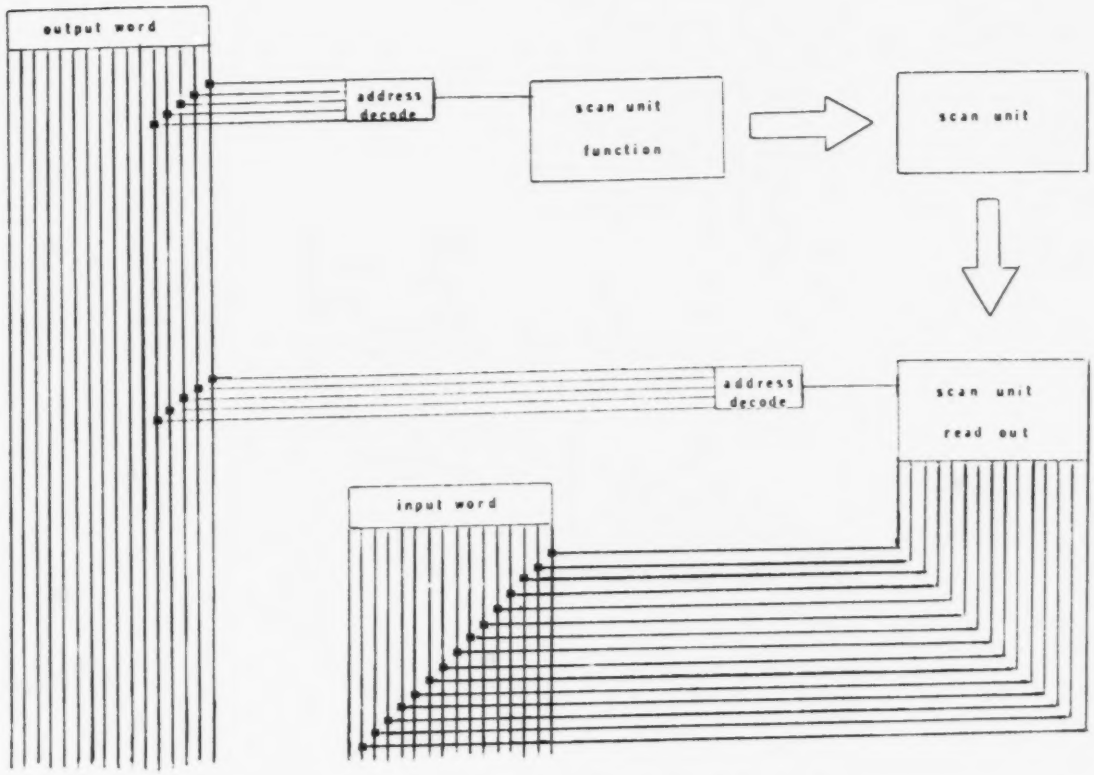

27 Simplified schematic of the basic operation of the scan unit interface. Both the input and output ports of the DR11k were required for communication with the computer .

nand gates in which one input was the address decode and the other the actual data being sent to the computer. Those from the scan unit were BCD outputs of the wavelength of the dye laser.

The stepping motor interface is also controlled by the DR11 I/O port. This interface consist of two operations: control and status monitoring. The general scheme for this interface is shown in Figure 28. The information that is required to make a particular stepping motor run is the address of that motor, the number of steps to be made and the direction in which to step. Thus a single output word can run a stepping motor leaving the computer free for other operations. The run and limit status of a motor are monitored by the status card and sent to the computer through the input word.

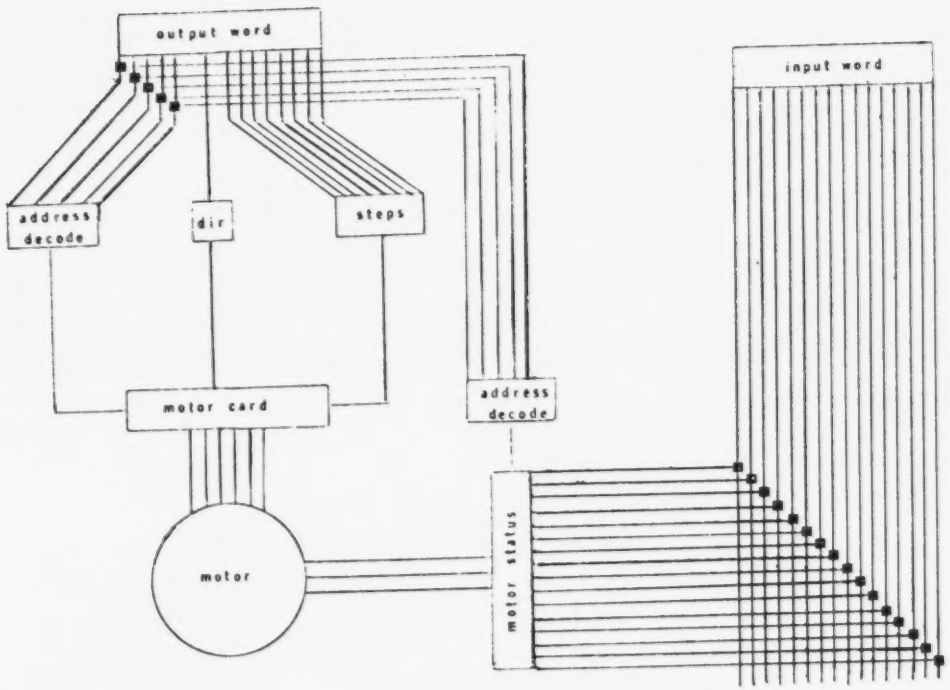

28 Simplified schematic of the basic operation of the stepping motor interface. The DR11C I/O port was used for controlling this interface.

The stepper control card can operate in one of two possible modes, local and computer. Part A of Figure 29 depicts a simplified scheme of what is involved in the local mode. The operations that are controlled are run (free run), direction (clockwise or counter clockwise),and step (single step). The run switch turns on an oscillator that puts out a pulse train to the motor either in the clockwise or counter clockwise direction. The step switch puts a single pulse to the motor. If a limit has been reached by the stepping motor, a micro switch for that direction is shorted to ground blocking the pulse train at the three-input nand gate. The computer mode of operation is depicted in Part B of Figure 29 and operates in the following manner. An output word containing the address, direction,and number of steps is put on the output bus. The address decodes allowing a binary up-down counter to be loaded. The counter is used only in the down count mode for this interface. Once the counter has been loaded, an external oscillator is switched on and a pulse train sent to the count down of the counter. The binary counter counts the number loaded down with its output being first coupled with the direction and

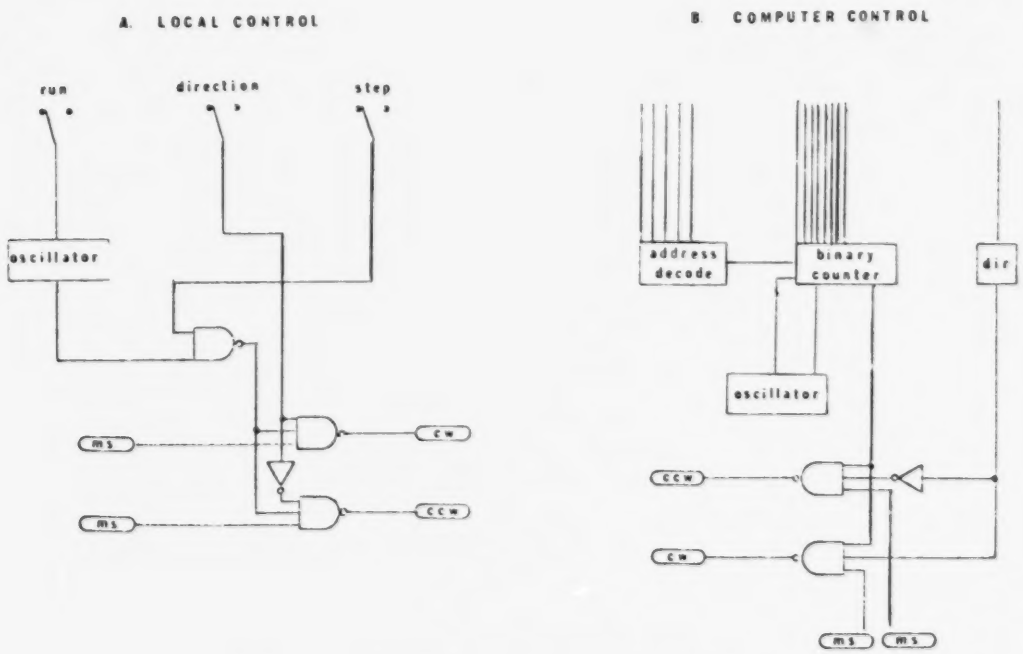

29 More detailed schematic of the stepping motor interface under local and computer control.

then sent to the motor. The maximum number of steps that can be loaded at one time is 200 (one revolution). The actual circuit that was used is shown in Figure 30. The run signal of each motor is monitored by the motor status card. When the correct address is given, the information is sent to the input port and subsequently to the computer. The micro switches are not individually monitored but monitored collectively. This is accomplished by an eight-input nand gate. If a limit is reached by a motor, program control can stop all operations and ring a bell, warning the user that a limit has been reached.

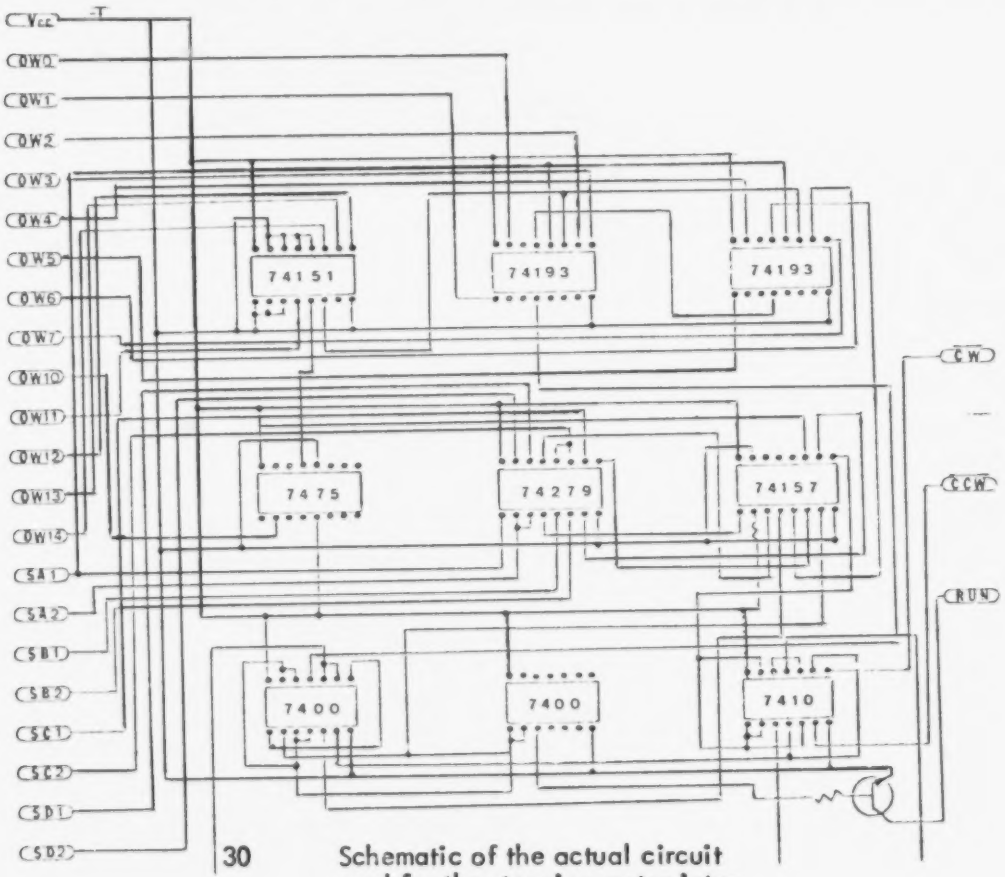

30 Schematic of the actual circuit used for the stepping motor interface. The symbols are: OWØ - output word bit Ø, SA - computer/ local switch, SB - direction switch, SC - scan switch, SD - single step switch, OSC - oscillator, MS1 - limit micro-switch for the CW direction and RUN turns on an external oscillator.

Using this hardware, complete automation of the CARS instrument has been achieved.

With the liquid chromatograph, U-V visible spectrometer and CARS instrument under computer control, software was developed to affect the separation, detection and identification of compounds. The first demonstration of the automated LC-CARS instrument was conducted for several chemists from the Environmental Research Laboratory, Athens, Georgia. Using a mixture of two model compounds: β-carotene and N-N diethyl paranitrosoaniline. The entire process was conducted under computer control: chromatographic fractionation, UV-visible detection and spectral scan, and CARS spectrum.

REFERENCES

1. G. A. Junk, J. J. Richard, M. D. Grieser, D. Witiak, J. L. Witiak, M. D. Arguello, R. Vick, H. J. Svec, J. S. Fritz, and G. V. Calder, J. Chromatog., 99 (1974) 745-762.
2. J. J. Lichtenberg, FCB Newsletter, Aug. 20 (1970).
3. B. Ahling and S. Jensen, Anal. Chem., 42 (1970) 1483.
4. W. E. May, S. N. Chesler, S. P. Cram, B. H. Gump, H. S. Hertz, D. P. Enagonio, and S. M. Dyszel, J. Chromatogr. Sci., 13 (1975) 535.
5. J. J. Kirkland, Anal. Chem., 43 (1971) 37A.
6. Application Highlights No. 24-PCB's, Waters Associates, Framingham, Mass., 1972.
7. J. A. Schmit, R. A. Henry, R. C. Williams, and J. F. Dreckman, J. Chromatogr. Sci., 9, 645 (1971).
8. R. E. Majors, American Lab., October (1975).
9. J. A. Armstrong, N. Bloembergen, J. Ducuing, and P. S. Pershan, Phys. Rev., 127, 1918 (1962).
10. P. D. Maker and R. W. Terhune, Phys. Rev., A137, 801 (1965).
11. J. J. Wynne, Phys. Rev. Lett., 29, 650 (1972).
12. E. Yablonovitch, C. Flytzanis, and N. Bloembergen, Phys. Rev. Lett., 29, 285 (1972).
13. M. D. Levenson, C. Flytzanis, and N. Bloembergen, Phys. Rev., B6, 3962 (1972).
14. P. R. Regnier and J. P. E. Taran, Appl. Phys. Lett., 23, 240 (1973).
15. M. D. Levenson, IEEE J. Quantum Electron., QE-10, 110 (1974).
16. M. D. Levenson and N. Bloembergen, J. Chem. Phys., 60, 1323 (1974).
17. R. F. Begley, A. B. Harvey, and R. L. Byer, Appl. Phys. Lett., 25, 387 (1974).
18. R. F. Begley, A. B. Harvey, R. L. Byer, and B. S. Hudson, J. Chem. Phys., 61, 2466 (1974).

19. R. F. Begley, A. B. Harvey, R. L. Byer, and B. S. Hudson, Am. Lab., 6(11), 11 (1974).

20. I. Itzkan and D. A. Leonard, Appl. Phys. Lett., 26, 106 (1975).

21. F. Mova, S. A. J. Druel, and J. P. E. Taran, Opt. Commun., 13, 169 (1975).

22. J. J. Barrett and R. F. Begley, Appl. Phys. Lett., 27, 129 (1975).

23. I. Chabay, G. K. Klauminzer, B. S. Hudson, Appl. Phys. Lett., 28, 27 (1976).

24. A. C. Albrecht, J. Chem. Phys., 34, 1476 (1961).

25. J. Tang and A. C. Albrecht, in "Raman Spectroscopy," Vol. 2 (H. A. Szymanski, Ed.), Plenum Press, New York, 1970, and references cited therein.

26. B. Hudson, W. Heatherington, III, S. Kramer, I. Chabay, and G. K. Klauminzer, Proc. Natl. Acad. Sci. (in press).

27. F. Inagaki, M. Tasumi, and T. Miyazawa, J. Mol. Spectrosc., 50, 286 (1974).

28. L. Rimari, R. G. Kilponen, and D. Gill, J. Amer. Chem. Soc., 92, 3824 (1970).

29. J. E. Davis and E. D. Schmidlin, Chem. Inst., 4, 169 (1973).

COLLABORATORS

FACULTY

T. B. Malloy (Mississippi State University)
J. D. Stuart (University of Connecticut)
R. von Wandruszka (University of Georgia)

POSTDOCTORAL RESEARCH ASSOCIATES

R. M. Irwin
G. W. Martin
P. K. Tseng

GRADUATE STUDENTS

R. R. Antcliff
L. P. Goss

PUBLICATIONS

1. "Excitation Profiles for the Coherent anti-Stokes Raman Spectrum of Beta Carotene," L. A. Carreira, T. C. Maguire and T. B. Malloy, Jr., J. Chem. Phys., 66, 2621 (1977).

2. "Microsampling and the Use of a Flow Cell for Coherent Anti-Stokes Raman Spectroscopy (CARS)," L. B. Rogers, J. D. Stuart, L. P. Goss, T. B. Malloy, Jr., and L. A. Carreira, Anal. Chem., 49, 959 (1977).

3. "On the Possibility of Coherent Anti-Stokes Raman Spectroscopy in the UV," L. A. Carreira, L. P. Goss, and T. B. Malloy, Jr., J. Chem. Phys., 66, 2762 (1977).

4. "Experimental Evidence on the Source of Negative Peaks in Coherent Anti-Stokes Raman Spectra," L. A. Carreira, L. P. Goss, and T. B. Malloy, Jr., J. Chem. Phys., 66, 4360 (1977).

5. "Preresonance Enhancement of the Coherent Anti-Stokes Raman Spectra of Fluorescent Compounds," L. A. Carreira, L. P. Goss, and T. B. Malloy, Jr., J. Chem. Phys., 68, 280 (1978).

6. "Raman Spectrum and Torsional Potential Function for Vinylcyclopropane," L. A. Carreira, T. G. Towns, and T. B. Malloy, Jr., J. Amer. Chem. Soc., 100, 385 (1978).

7. "Comparison of the Coherent Anti-Stokes and Coherent Stokes Raman Lineshapes of the ν_1 Line of Beta-Carotene Near a One Photon Resonance," L. A. Carreira, L. P. Goss, and T. B. Malloy, Jr., J. Chem. Phys., 69, 855 (1978).

8. "Coherent Anti-Stokes Resonance Raman Spectra of Highly Fluorescent Compounds," L. A. Carreira, Advances in Laser Chemistry, A. H. Zewail, ed., Springer Series in Chemical Physics, Springer, Berlin, Heidelberg, New York, 1978.

9. "Conformational Barriers and Interconversion Pathways in Some Small Ring Compounds," T. B. Malloy, Jr., L. E. Bauman, and L. A. Carreira, Topics in Stereochemistry, N. L. Allinger and Ernest L. Eliel, editors, 1978.

10. "Low-Frequency Vibrations in Small Ring Compounds," L. A. Carreira, R. C. Lord, and T. B. Malloy, Jr., Springer-Verlag Publishing Co., Heidelberg, Germany, 1978.

11. "Resonance Enhanced CARS," L. A. Carreira, Proceedings of the Sixth International Raman Conference, 1978.

12. "Effect of a Change in Solvent on Chromatographic Peak Shapes," Paul K. Tseng and L. B. Rogers, J. Chromatogr. Sci., 16, 436 (1978).

13. "Retention Behavior of Dinitrobenzene Isomers and Dihydroxybenzene Isomers on Octadecyl and Phenyl Bonded Phase Packings," Paul K. Tseng, J. Chromatogr. Sci., 16, 438 (1978).

14. "Coherent Anti-Stokes Resonance Raman Excitation Profiles of Tetracene," L. A. Carreira, T. C. Maguire, and T. B. Malloy, Jr., J. Chem. Phys., 00, 0000 (1979).